Infection

P. Agarwal, L. Romano, H. Prosch, and G. Schueller

Contents

P. Agarwal • H. Prosch
Department of Biomedical Imaging and Image-guided
Therapy, Vienna General Hospital, Medical University
of Vienna, Währingergürtel 18-22, 1090 Vienna,
Austria

L. Romano
Department of Emergency Radiology,
Cardarelli Hospital, Naples, Italy

G. Schueller (✉)
Assoc. Prof. Dr. Gerd Schueller MBA, Academic Health,
Rietgrabenstrasse 76b, CH-8152 Opfikon, Switzerland

1   Community-Acquired Pneumonia

1.1   Introduction

Community-acquired pneumonia (CAP) is a frequent lower respiratory tract infection.

It is highly influenced by the geographic area and the population.

The microorganisms may reach the lower respiratory tract from inhaled air or from infected oropharyngeal secretions (Vincent et al. 1995). Droplet transmission from human to human is another usual mode of spread of the pulmonary infection, especially in immunocompetent patients and young children.

Clearance by mucociliary system can filter infective organisms 5–10 nm in diameter, so that microorganisms between 1 and 2 nm can reach the alveolar tissue. The alveolar infection depends on the balance between the virulence of the microorganism and body defenses due to cellular phagocytosis. There are several factors

predisposing to the development of CAP as cardiovascular diseases, diabetes, uremia, immunodeficiency, obstructive pulmonary chronic disorders with mucociliary clearance insufficiency, and age.

Alcoholic patients and people with poor oral hygiene are particularly sensitive to develop pulmonary infections (Barlettand Finegold 1974).

The clinical presentation of pneumonia is frequently represented with sudden symptoms as high fever, cough, purulent expectoration, and deep chest pain. Neutrophilia is common.

CAP is classified into three main groups: lobar pneumonia, bronchopneumonia, and interstitial pneumonia (Bhalla and Mc Loud 1998).

Lobar pneumonia appears in the lung parenchyma periphery and then diffuses up to the hilum. It is generally limited to one pulmonary segment or lobe.

Bronchopneumonia occurs when infectious microorganisms produce acute bronchial mucosal inflammation and spread through the airway into the alveolar spaces determining pulmonary consolidation.

Interstitial pneumonia is determined by the infection of pulmonary interstitium and is mainly caused by viral organism.

The same organism may produce several different patterns that depend on the balance between the microorganism charge and the body immunity defenses.

The spectrum of bacteria responsible for CAP includes *Streptococcus pneumoniae*, *Haemophilus influenzae*, *Staphylococcus aureus, Mycoplasma pneumoniae, Chlamydia pneumoniae, Legionella pneumophila,* and *Klebsiella pneumoniae* (American Thoracic Society 1995; Marom et al. 1999; De Paso 1991).

Among the types of CAP, *S. pneumoniae* is the most frequent causing bacteria, and it is associated with a high mortality rate in the elderly and childhood.

Haemophilus influenzae also is one of the most frequent bacteria causing CAP, because it frequently colonizes the human upper respiratory tract, especially the nasopharynx, and is considered to form part of the normal respiratory flora. It is also an important cause in the acute exacerbation of chronic obstructive pulmonary infectious disease (Kofteridis et al. 2009).
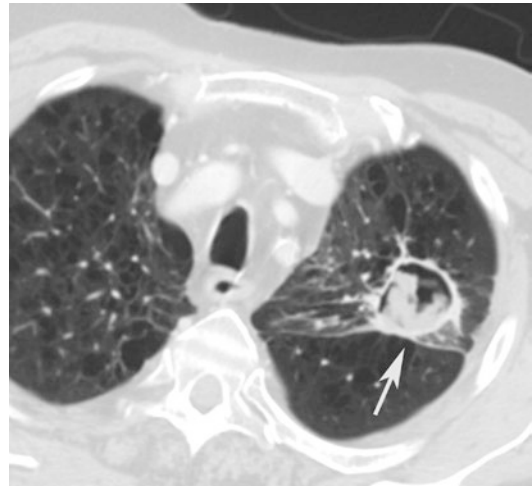

Fig. 1 Fungal abscess (*white arrow*) in diffuse pulmonary emphysema. Post-contrast CT axial scan demonstrates large air-containing dishomogeneous focal area, with peripheral-enhanced irregular wall, characteristic of fungal abscess, with underlying pulmonary emphysema

The viruses that most commonly cause pneumonia are respiratory syncytial virus, herpes simplex, parainfluenza virus, influenza virus, adenovirus, and cytomegalovirus.

The funguses that most commonly cause pneumonia are *Pneumocystis*, *Aspergillus*, and *Candida*.

Pulmonary emphysema and bronchiectasis are frequently seen in patients with CAP because chronic obstructive pulmonary disease is a predisposing factor for developing pulmonary infection (Reittner et al. 2000a) (Fig. 1).

1.2 Lobar Pneumonia

Depending on the severity of the pulmonary alveolar tissue involvement, the pattern of the infection may be patchy or homogeneous. The consolidation is usually confined to one lobe, although multilobar involvement is not uncommon (Fig. 2). Because the bronchial tree is not involved, there is no volume loss of the inflamed pulmonary segment or lobe.

Lobar pneumonia is characterized by the filling of alveolar spaces by edema full of white and inflammatory cells. The inflammation generally begins at the lung mantle and then diffuses to the entire lobe through Kohn pores and peripheral small

Fig. 2 Bilateral pneumonia. CT coronal scan demonstrates lobar consolidation of *right upper* and *lower lobes* with no volume loss and bulging of interlobar fissure. On the other side, there are lobular areas of consolidation. Air bronchograms within the consolidation areas are preserved
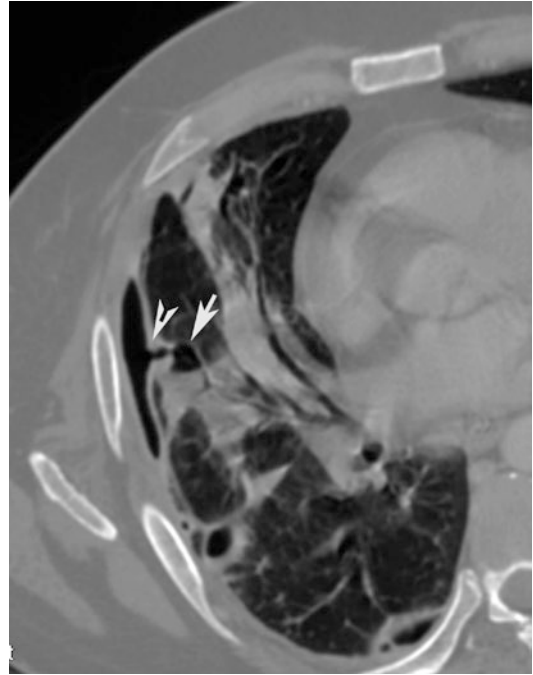

Fig. 3 Lung abscess. Post-contrast CT axial scan demonstrates large focal area of decreased attenuation with air-fluid level, with rim enhancement, characteristic of lung abscess (*arrow*) of the left upper lobe

Fig. 4 Post-contrast CT axial scan demonstrates a small air-containing pulmonary cavity with fluid level (*arrow*) ruptured into the pleural space (*arrow tip*) with a small left pneumothorax

airways; usually it is limited by an interlobar fissure. The air bronchograms within the consolidation area are preserved (Fig. 2). Nodular pneumonia is frequently caused by fungal infections and is prevalent in young or immunocompromised patients.

The pneumonia could be complicated with cavitation and abscess (Fig. 3), necrosis of the inflamed lung parenchyma, and loculated empyema (Muller et al. 2007).

Abscesses develop in up to 30 % of cases, are usually solitary, and typically have an irregular wall. They could rupture into the pleural space with the development of pneumothorax and empyemas (Fig. 4). Abscesses may also erode into bronchial tree and produce air-containing cavities with fluid levels. The consequent bronchial aspiration and diffusion of infection can determine patchy consolidation or nodules in dependent portions of both the lungs (Fig. 5). The consolidations are usually multilobar and bilateral in distribution.

A large solitary abscess or primary lung abscess can develop in a patient without underlying lung inflammation as a consequence of aspiration of oropharyngeal secretions in combination with impairment of systemic defense condition.

Necrotizing pneumonia, generally determined by Gram-negative bacteria, produces exfoliated pulmonary tissue within a cavity or diffuses microabscesses secondary to thrombosis of the vessel that supply the consolidation. Sometimes necrotizing pneumonia consists of a fulminant process associated with focal areas of necrosis that results in abscesses that can coalescence, resulting in large cavities that may exhibit thick fibrotic walls if they are chronic. There are large

Fig. 5 CT sagittal scan demonstrates multiple nodules in dependent portions of the lung

Fig. 6 Bronchopneumonia. CT coronal scan demonstrates multiple, bilateral, centrilobular nodules
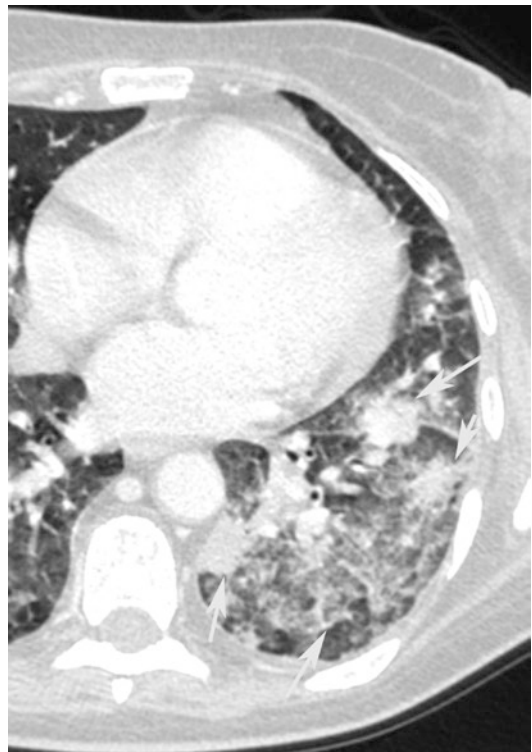
Fig. 7 Bronchopneumonia. CT axial scan demonstrates multiple, lobular (*arrow*), patchy, confluent consolidation areas of the left lower lobe

cavities with concomitant small cavities frequently associated with empyema (Winer-Muram et al. 1993). This feature is frequent in immunocompromised patients.

1.3 Bronchopneumonia

Bronchopneumonia or lobular pneumonia is characterized by a peribronchiolar inflammation with thickening of peripheral bronchial wall, the diffusion of inflammation to the centrilobular alveolar spaces, and development of nodules (Fig. 6). From the centrilobular tissue, the inflammation can spread to lobular (Fig. 7) or subsegmental areas giving a consolidation. The areas of consolidation may be patchy or confluent, multilobar, unilateral, or bilateral (Fig. 8). Because the process involves the airways, it can determine a loss of volume of the affected pulmonary segment (Ito et al. 2009).
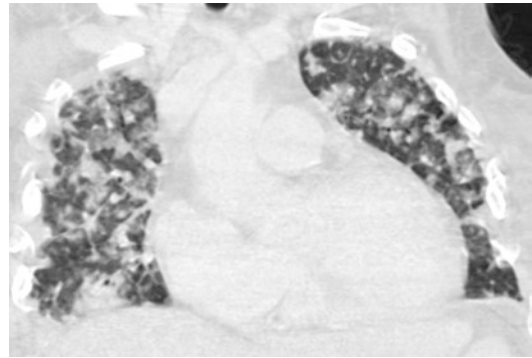
1.4 Interstitial Pneumonia

Interstitial pneumonia is frequently caused by virus.

The viral pneumonia begins with the destruction and exfoliation of the respiratory ciliated and
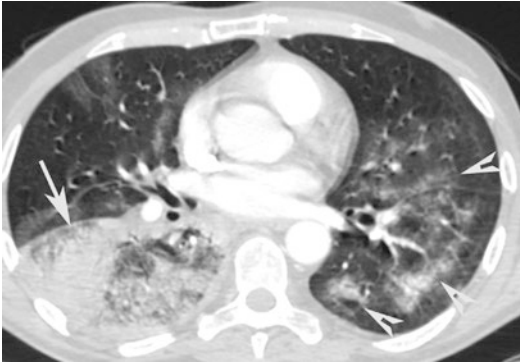
Fig. 8 Bronchopneumonia. CT axial scan demonstrates multiple confluent areas of consolidation (*arrow*) of the right lower lobe and patchy lobular areas of consolidation of the left lower lobe (*arrow tips*)
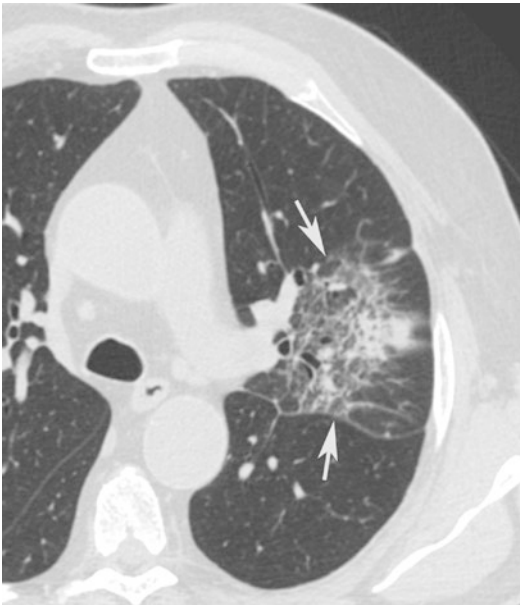

Fig. 9 Interstitial pneumonia. CT axial scan evidences that the lingular interstitial septa, bronchial and bronchiolar walls are thickened for an inflammation process (*arrows*). There is also a central lobular consolidation with patchy appearance

mucous cells. The interstitial septa and the bronchial and bronchiolar walls become thickened for the inflammation process and lymphocyte interstitial infiltrates (Fig. 9). The consequent interstitial pneumonia has often a patchy appearance, frequently with coalescence, involving predominantly the peribronchial portions of the

Fig. 10 Chest radiograph shows a right upper lobe opacity (*arrow tip*) and a nonhomogeneous consolidation of the right lower lobe (*arrow*)

pulmonary lobules (Shiley et al. 2010). With the progression of inflammation, the alveolar sacs fill with exudate that could be hemorrhagic. As consequence a hyaline membrane can develop in alveolar spaces.

The pneumonia can heal completely, but sometimes a chronic interstitial fibrosis can occur.

1.5 Radiographic Features

Chest radiography represents an important initial examination in all patients suspected of having pulmonary infection and for monitoring response to therapy.

Its role is to identify the pulmonary opacities (Fig. 10), their internal characteristics and distribution, pleural effusion, and presence of other complications as abscesses and pneumothorax.

Radiographic manifestations depend on the immune status of the patient and the presence of preexisting lung chronic alterations as emphysema, chronic bronchitis, and bronchiectasis and vary somewhat among the various species of causing microorganisms.

The most common radiographic findings include hazy ground-glass opacities, confluent or patchy airspace consolidations, cavitations, and
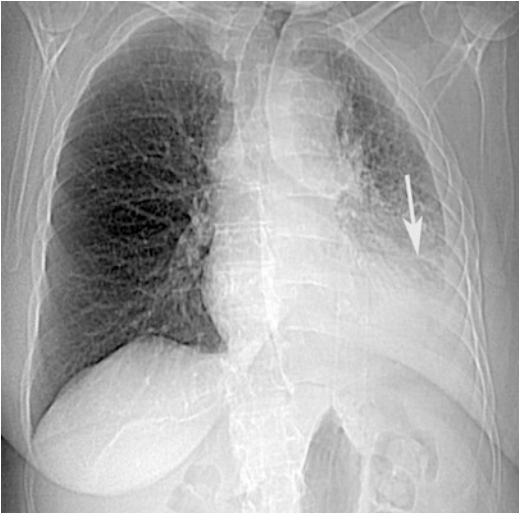
Fig. 11 Posteroanterior chest radiograph shows dense left lower lobe airspace consolidation (*arrow*) with pleural fluid

poorly defined linear or reticular-nodular opacities (Chastre et al. 1998).

These alterations may involve mainly the perihilar regions, lower lung zones, or upper lung zones. They are usually unilateral but may involve both lungs. Other findings are pleural effusion and hilar adenopathy.

In some cases, the radiographic findings are suggestive or consistent with the diagnosis of pneumonia and are sufficiently specific in proper clinical context to preclude the need for additional imaging (Fig. 11) (Franquet 2001).

However, the bedside plain film, the projection effects, and the poor density resolution frequently limit the value of radiography as a diagnostic tool. Radiographic features are sometimes nonspecific, and the relatively low diagnostic accuracy of chest radiography can be improved with CT.

1.6 Computed Tomography Findings

CT has been shown to be more sensitive than x-ray plain film and provide additional information that affects diagnosis or management in up to 70 % critically ill patients (Heussel et al. 1997).

High resolution CT allows accurate assessment of airspace inflammation (Okada et al. 2012).

The distribution of parenchymal alterations is based on the evidence of their localization at CT scan. If the primary opacity is predominantly located in the inner third of the lungs, the pathology is classified as having a central distribution. A peripheral opacity is defined as a lesion localized in the outer third of the lungs. Zonal predominance is classified as either upper or lower. In the upper lung zone predominance, the alteration is located above the level of the tracheal carina, whereas in the lower zone predominance, it is located below the upper zone.

The CT findings include nodules, interlobular septal thickening, intralobular reticular opacities, ground-glass opacities, tree-in-bud pattern, lobar-segmental consolidation, lobular consolidation, abscesses, pneumatocele, pleural effusion, pericardial effusion, mediastinal and hilar lymphadenopathies, airway dilatation, and emphysema.

Nodules measure from 3 to 10 mm and are divided into three types: centrilobular nodules that are small nodules in centrilobular location, peribronchovascular nodules that are relatively larger nodules associated with the peribronchovascular bundle, and "random nodules" that are not associated with centrilobular structures or bronchovascular bundle.

The centrilobular nodules reflect a peribronchial inflammation with a centrilobular distribution (Fig. 12).

They are defined as a dot-like opacities localized inside the center of a secondary pulmonary lobule. They are present around the peripheral pulmonary arterial branches or 3–5 mm from the pleura, interlobular septa, or pulmonary veins.

Nodules that are present in the bronchovascular bundle are called peribronchovascular nodules (Fig. 13).

Hemorrhagic pulmonary nodules have a central area of soft tissue attenuation surrounded by a halo of ground-glass attenuation (Primack et al. 1994).

Pulmonary hemorrhage in association with nodules occurs in patients with herpes simplex virus, candidiasis, and cytomegalovirus pneumonia (Thurlbeck et al. 1991)
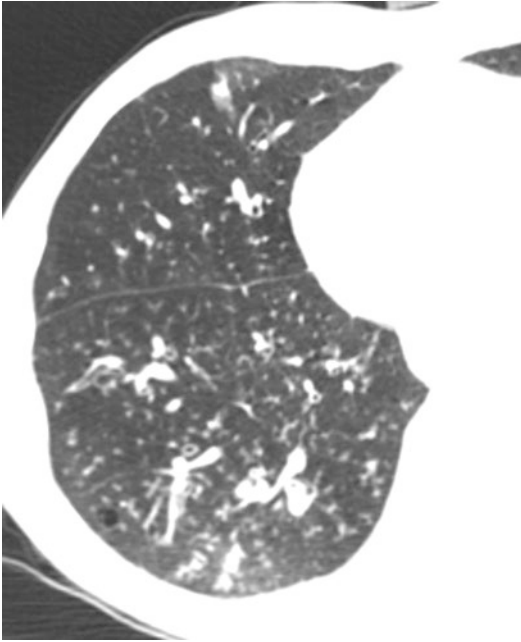
Fig. 12 CT axial scan evidences multiple centrilobular nodules and peribronchial inflammation with centrilobular distribution

Fig. 13 Peribronchovascular nodules. CT sagittal scan shows small nodules (*arrow tips*) in the bronchovascular bundle and peribronchial inflammation (*arrows*)

Fig. 14 CT sagittal scan shows small nodules (*arrow tips*) associated with thickening of the bronchovascular structures (*arrow*)

Interlobular septal thickening are defined as abnormal widening of the interlobular septa. Intralobular reticular opacity is considered to be present when interlacing line shadows are separated by a few millimeters (Fig. 9) (Austin et al. 1996).

It is frequently associated with bronchial wall thickening. Thickening of the bronchovascular structures is defined as an apparent thickening of the bronchovascular bundle in comparison with the unaffected lung parenchyma (Fig. 14).

Ground-glass opacity was defined as hazy increased opacity with preservation of bronchial and vascular markings (Fig. 15). It is present particularly in pneumocystis and cytomegalovirus infections (Fig. 16).

Tree-in-bud pattern may be seen in a variety of bacterial, mycobacterial, fungal, and viral infections and consists of centrilobular branching tubular structures, bronchovascular bundle
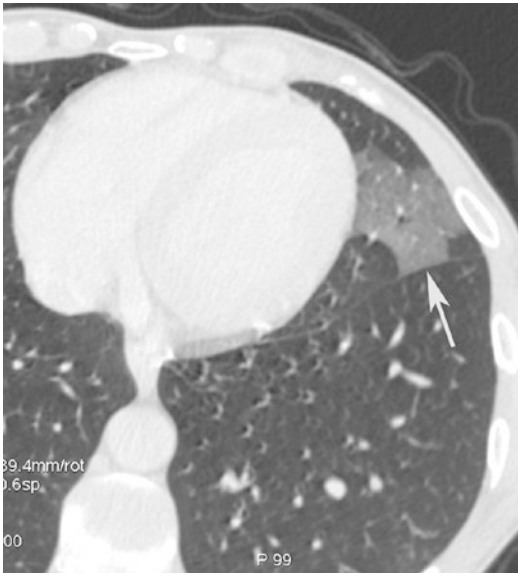
Fig. 15 Ground-glass opacity. CT axial scan evidences a lingular ground-glass opacity (*arrow*) with preservation of bronchial and vascular markings

Fig. 16 CT axial scan demonstrates multiple, confluent, bilateral ground-glass opacities with preservation of bronchial (*arrow tip*) and vascular (*arrow*) markings

thickening, and nodules and reflects the presence of bronchiolar inflammation and filling of the bronchiolar lumen by inflammatory exudate (Fig. 17) (Aquino et al. 1996).

Airspace consolidation is considered to be present when homogeneous increases in pulmonary parenchymal attenuation obscured the margins of vessels and airway walls (Fig. 2) (Hansell et al. 2008).

Fig. 17 Tree in bud. CT axial scan demonstrates centrilobular branching tubular structures, bronchovascular bundle thickening, nodules that reflect the presence of bronchiolar inflammation, and filling of the bronchiolar lumen by inflammatory exudate

The CT findings in viral pneumonia are based on the evidence of small patchy opacities that can coalescence (Fig. 18), composed of multiple, poorly defined 2–3 mm nodules; multilobar involvement is frequent. Bronchial wall and peribronchial thickening frequently spread outward from the hila. Hilar adenopathy and pleural effusion are common.

The abscess can drain into a bronchus that leads to the classic air-fluid level, present in up to 72 % of cases (Fig. 3). The complete drainage of the cavity can lead to a pneumatocele.

Pneumatocele is a frequent consequence of an abscess drained in the lumen of a bronchus; it is a gas-filled area with a thin wall that may increase and can get ruptured into the pleural space, causing a pneumothorax. It can also heal completely, fading from the periphery to form a tiny thin-walled air-cyst or a linear scar.

Pleural effusion is better detected with CT than with radiography and is often associated with a high risk of empyema that requires prompt early drainage.

Fig. 18 Viral pneumonia CT axial scan evidences small patchy opacities of the left lower lobe

Fig. 19 Pulmonary abscess associated with purulent pericarditis. Post-contrast CT axial scan demonstrates a pre-pericardial lung abscess (*arrow tip*) of the left lower lobe associated with thickening of the pericardium and pericardial effusion (*arrow*)

Purulent pericarditis is a relatively rare and a rapidly fatal complication of pneumonia. The consequent development of cardiac tamponade may be rapid. At the beginning, heart size may be normal at chest radiograph, whereas CT can demonstrate early the pericardial effusion that requires prompt drainage for avoiding cardiac compression (Fig. 19) (Naidich et al. 1983).

Mediastinal and hilar lymphadenopathies are evaluated when the minimal diameter of a lymph node is larger than 10 mm. Lymph node enlargement is very frequent in pneumonia and generally involves the paratracheal, tracheobronchial, and subcarinal mediastinal chains.

Airway dilatation predisposes to pneumonia and is considered to be present if the bronchial size exceeded that of the near pulmonary artery.

Pulmonary emphysema is frequently associated with pneumonia and is defined as scattered or diffuse areas of low attenuation without internal vascular structures in comparison with normal pulmonary parenchyma (Fig. 1).

1.7 Conclusion

Pneumonia is the first leading cause of death due to infection worldwide (Vilar et al. 2004a).

Many Gram-positive, Gram-negative bacteria, funguses, and viruses can cause the infectious pulmonary disease, and the severity of pneumonia depends on the balance between the microorganism charge, the body immunity defenses, and the quality of the underlying pulmonary tissue.

Among the types of CAP, *S. pneumoniae* is the most frequent causing bacteria, has a tendency to develop antibiotic resistance, and is associated with a high mortality rate in the elderly and childhood (Musher et al. 2002).

Radiographically pneumonia is divided into three patterns: lobar pneumonia, bronchopneumonia, and interstitial pneumonia (Muller et al. 2007).

Chest x-ray film is routinely performed for the initial evaluation of patients with suspect pulmonary infection, and it is considered the recommended tool for the diagnosis of CAP. However, chest x-ray film not always evidences all the findings of pneumonia, and it is limited by the interobserver variability in interpretation.

Especially in not clear or even negative chest radiography pattern, in patients with clinical symptoms, CT is recommended, for its high

spatial resolution and the ability to evidence very early and minimal pulmonary alterations indicative of pneumonia.

2 Atypical Infections

2.1 Definition

Community-acquired pneumonias have been traditionally divided into "typical" and "atypical" pneumonias. The main aim of such a classification was to help the clinician narrow the differential diagnosis and choose an appropriate therapy based on the likely offending organism (Murray and Mason 2010).

Typical pneumonia is characterized by infection with bacteria such as *Streptococcus pneumoniae*, *Klebsiella pneumoniae*, and *Haemophilus influenzae*. It presents with symptoms such as acute onset of high grade fever with chills, cough with purulent expectoration, and pleuritic chest pain. Further evaluation of these patients reveals an elevated white blood cell count, elevated CRP, and lobar or segmental consolidation on imaging studies (Murray and Mason 2010).

Atypical pneumonia, as the name explains, does not show these *typical* features. An early use of this term in the literature dates back to 1938 when cases of patients who presented with milder symptoms and protracted course came to notice (Reimann 1938). These patients had more generalized symptoms like malaise, body pains, and low-grade fever with dry cough and flu-like symptoms. The causative organism could not be cultivated on regular media or stained with regular staining methods. Mycoplasma was first isolated in 1944 and was attributed as the etiology of primary atypical pneumonia (Eaton et al. 1944). However, several other organisms cause atypical symptoms.

Although originally used to signify any infection that was unusual in presentation, atypical pneumonia is now a broad term that includes infections caused by common organisms like *Mycoplasma pneumoniae*, *Chlamydia pneumoniae*, and *Legionella pneumophila* and viruses

(Marrie et al. 1981). Atypical, however, does not mean that they are rare; they account for almost 15–20 % of the cases of CAP (Arnold et al. 2007). *Mycoplasma pneumoniae* is the most common cause of atypical pneumonia followed by *Chlamydia pneumoniae* and *Legionella pneumophila* (Arnold et al. 2007). Apart from these conventional pathogens, there are emerging infections with newer organisms like *Hantavirus*, human metapneumovirus that can also cause atypical pneumonia. In view of the current radiological discussion and similar radiological appearances shared by mycoplasma and various viruses, we will also be discussing some additional infections in this chapter, which, although not considered routinely under the heading of "atypical pneumonia," are atypical enough to justify their inclusion here.

2.2 General Features

Infections with many, if not all, atypical organisms share some common features. Mycoplasma, chlamydia, and viruses have many similarities in their pathology, clinical, and radiological features. Grossly, these pathogens cause predominant histological changes in the respiratory epithelium and in the peribronchial interstitium (Müller et al. 2007; Müller 2003). The ensuing bronchiolitis and alveolitis are characterized by infiltration of the epithelium with mononuclear cells and presence of neutrophilic exudate in the lumen of the airways. These changes are predominantly seen in the terminal and respiratory bronchioles and manifest radiologically as peribronchial nodules (Müller et al. 2007; Müller 2003).

Bronchiolitis with exudate in the lumen of the airways is seen on radiographs as reticulonodular pattern and on CT as tree-in-bud nodules. As the nodules enlarge, they involve the entire secondary pulmonary lobule and are seen as "lobular" consolidation: these features are typical of bronchopneumonia pattern. Further extension into segmental and patchy lobar consolidation may be seen in advanced stages, and this may be difficult to distinguish from bacterial infection. Partial

filling of the airways gives rise to ground-glass opacities (Müller et al. 2007).

Some infections like influenza and hantavirus cardiopulmonary syndrome, on the other hand, cause rapidly progressive pneumonia with diffuse alveolar damage (Kim et al. 2002).

The clinical course of atypical pneumonias is generally subacute, the WBC counts are generally normal, and the imaging features are heterogeneous and nonspecific.

2.3 Radiological Aspects

Diagnosis of pneumonia requires a combination of clinical, microbiological, and radiological features. Chest radiograph is usually sufficient to confirm the diagnosis. It also helps in follow-up of the patients and evaluation of the response to treatment. CT scans are not routinely recommended but are helpful in case of doubtful features on chest radiographs, when no adequate response to the treatment is noted and when complications or underlying pathology is suspected (Vilar et al. 2004b). CT scan can be further helpful in suggesting an etiological diagnosis. In indeterminate cases, CT-guided procedures come in as problem-solving tools for the correct diagnosis.

2.4 Bacteria

2.4.1 Mycoplasma Pneumonia

Mycoplasma pneumoniae is a common cause of community-acquired pneumonia, particularly in young children. It is the smallest free-living organism, measuring approximately 125–150 microns in size which is similar to that of myxovirus (Marrie et al. 2012). Lack of cell wall makes them highly pleomorphic.

Mycoplasma pneumoniae was first isolated from the sputum of a patient with "atypical pneumonia" by Eaton et al. and was initially considered to be a virus due to its ability to pass through bacterial filters. Subsequent studies led to its identification as bacteria (Cunha 2010).

Mycoplasma pneumonia is commonly seen in young children and adolescents and shows a declining incidence in adults (Meyer Sauteur et al. 2016). It spreads through droplet spread or direct contact. The incubation period is around 1–2 weeks (John et al. 2001).

Clinical symptoms resemble a viral infection and are characterized by mild symptoms like dry cough, headache, malaise, and low-grade fever (John et al. 2001). In view of these mild symptoms, it is also called as "walking pneumonia" (Meyer Sauteur et al. 2016). However, sometimes severe infection and extrapulmonary manifestations may also be seen. In one study by Marrie et al., common extrapulmonary manifestations were thrombocytosis, hemolysis, Guillain-Barré syndrome, and pulmonary hemorrhage (Marrie et al. 2012). In asthmatic patients, it can cause an acute exacerbation of asthma and present with acute dyspnea.

Typically, the WBC counts remain in the normal range. A secondary bacterial infection is likely when they are elevated (John et al. 2001).

An attempt to suggest the offending organisms on radiology can be worthwhile for two main reasons: firstly, infection with these cell wall-deficient bacteria calls for treatment with antibiotics other than the usual cell wall synthesis inhibitors like penicillin, which are otherwise suitable for typical infections with pneumococcus. Laboratory tests take time, pending, which a radiological diagnosis can prove helpful in clinical decision making. Secondly, in appropriate settings, radiological features, although not highly specific, can be suggestive of the diagnosis in many cases.

The chief pathology is acute cellular bronchiolitis with bronchial wall inflammation, peribronchial infiltrates of lymphocytes and macrophage, and intraluminal exudative fluid (Pipavath et al. 2005; Muller and Miller 1995). This is seen radiologically as thickening of bronchial wall and centrilobular nodules.

Radiographic features of mycoplasma are generally nonspecific and resemble viral pneumonias closely. Reticulonodular infiltrates in one or more lobes are seen on radiographs (John et al. 2001) (Fig. 20). Various studies have highlighted lower lobe predominance (John et al. 2001; Guckel et al. 1989). Bilateral peribronchial
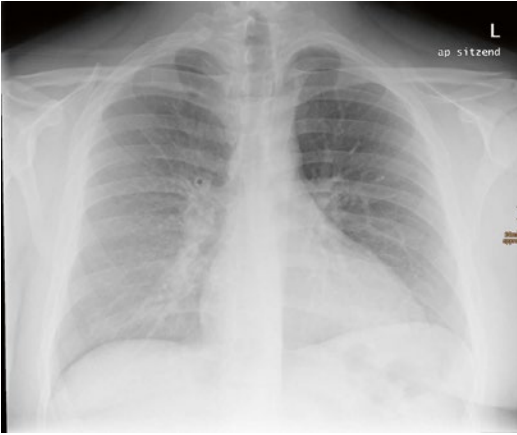
Fig. 20 A 21-year-old man with mycoplasma pneumonia: chest radiograph showing enlarged left hilar shadow. Reticulonodular opacities in the right lower lung field
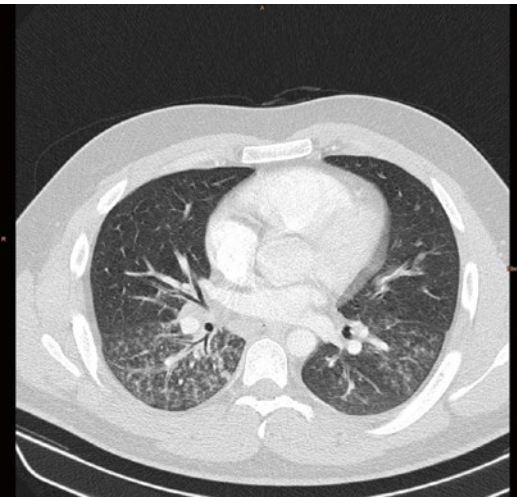

Fig. 21 Same patient as in Fig. 20: CT scan showing centrilobular nodules, tree-in-bud, and bronchial wall thickening in both lower lobes

infiltrates may also be seen. Patchy consolidation may be seen; however, dense lobar consolidation as in typical bacterial pneumonias is less likely (Eaton et al. 1944).

Mycoplasma pneumoniae pneumonia presents itself on computed tomography (CT) like bronchopneumonia. Centrilobular nodules are the most common findings on CT (Reittner et al. 2000b) (Fig. 21). They coalesce and form consolidations. Consolidations and ground-glass opacities with patchy involvement of the

secondary pulmonary lobules and interspersed sparing of some lobules are typical (Reittner et al. 2000b). A combination of bronchial wall thickening and centrilobular nodules with bronchopneumonia can be highly suggestive of mycoplasma. CT helps to demonstrate the nodules and bronchial wall thickening better than radiographs, thereby helpful in pointing toward the diagnosis. Pleural effusions are less commonly encountered, seen in around 20 % of the cases, and when present are transient (John et al. 2001; Hsieh et al. 2007).

2.4.2 *Chlamydia pneumoniae*

Chlamydias are obligate intracellular bacteria that possess a cell wall. They exist in two forms: a smaller extracellular elementary body and a larger intracellular form called the reticulate body (Webb et al. 2011). Three species of chlamydia area known:

Chlamydia trachomatis typically causes ocular infection (trachoma) and sexually transmitted disease but may cause pneumonia in infants who are born to infected mothers.

Chlamydia psittaci is a pathogen in birds (causing psittacosis) and may cause respiratory infections in humans. The mode of infection is through aerosols containing bacteria generated from infected birds (Knittler and Sachse 2015).

Chlamydia pneumoniae was the third species to be discovered, first isolated in 1968 during trachoma vaccine trail and accounts for an estimated 10 % of the CAP cases (Kuo et al. 1995). It is a common cause of atypical pneumonia.

Transmission of infection occurs through respiratory secretions. Incubation period is several weeks.

Symptoms tend to be protracted and are subacute in onset. Prolonged cough and low-grade fever are typical features. Initial prodromal phase of upper respiratory tract symptoms like pharyngitis and hoarseness of voice are not uncommon.

The infection is typically mild, and extrapulmonary symptoms are less common in comparison to mycoplasma infection. It has also been implicated in coronary artery disease.

CT features consist of bronchopneumonia with consolidation, GGO, peribronchial

thickening, and nodules, similar to mycoplasma infection. However, pleural effusions are more common in patients with *Chlamydia pneumoniae*, bronchial wall thickening and centrilobular nodules more common in mycoplasma infection (Okada et al. 2005). Some studies described increased prevalence of emphysema and bronchial dilatation in *Chlamydia pneumoniae* pneumonia; COPD is an important risk factor for chlamydia (Hahn 1999; Karnak et al. 2001).

2.4.3 *Legionella pneumophila*

Legionella pneumonia is an atypical pneumonia, first discovered in 1976 due to an outbreak in a convention in Philadelphia (Fraser et al. 1977). The source of infection was later narrowed down to the cooling system of the air conditioner with circulating water which acts like a conducting medium for the bacteria.

It is a Gram-negative obligate intracellular bacterium that is a parasite of freshwater protozoans. It tends to colonize in various water facilities and causes outbreaks of infection when aerosols containing the bacteria are inhaled (Fields et al. 2002). In humans, it infects the macrophages, where it resides and multiplies.

Legionella pneumophila is described to cause two diseases: Legionnaires' disease which is a severe multisystemic infection and pneumonia with a long incubation period from 2 to 10 days and Pontiac fever which is a mild clinical illness with flu-like symptoms and a short incubation period of 36 h. *Legionella pneumophila* serogroup 1 accounts for most of the cases (Fields et al. 2002).

Legionnaires' disease varies from mild to severe disease requiring ICU care. It tends to cause electrolyte abnormalities, typically hyponatremia and hypophosphatemia, the presence of which must raise the suspicion of this infection. Presenting symptoms are usually constitutional like fever, myalgias, headache, confusion, and diarrhea which are seen early in the course of the disease, and then nonproductive cough appears later (Tsai et al. 1979).

Radiological features are usually nonspecific and resemble bacterial lobar pneumonia.

Radiographs show patchy peripheral consolidations initially. Airspace consolidation due to alveolitis is typical. Bilateral, multilobar, and multisegment consolidation and ground-glass opacities are the most common radiological features on CT (Yagyu et al. 2003). Centrilobular nodules and diffuse peribronchial thickening characteristic of mycoplasma and chlamydia are less commonly encountered in legionella (Kim et al. 2007). Cavitation may be seen occasionally in immunosuppressed individuals and patients on high steroids (Fairbank et al. 1991). Pleural effusions are seen in up to half of the patients and are usually mild or moderate. Delayed clearing up of the infiltrates and residual fibrosis may occasionally be seen.

2.5 Viruses

Lower respiratory tract infections can be caused by various viruses, and it is estimated that approximately 10 % of infections in CAP are due to viral etiology (ref). Along with the various radiological features, knowledge of the clinical history can be invaluable in narrowing the differential diagnosis. For example, in immunocompetent host, influenza virus is commonly implicated as an offender. In immunosuppressed individuals, however, the usual inciting organisms are herpes, cytomegalovirus, and adenovirus (Kim et al. 2002).

Viruses can be divided into (a) RNA viruses, myxoviruses (influenza, RSV, measles), coronavirus, and hantavirus, and (b) DNA viruses, adenovirus and herpes group including CMV and varicella zoster.

2.5.1 Influenza Virus

Influenza virus belongs to the family *Orthomyxoviridae* and is a single-stranded RNA virus. It has three predominant serotypes: influenza A, B, and C. Influenza A is responsible for majority of the epidemics and pandemics. Influenza virus A and B may cause pneumonia, while C causes only sporadic mild infections (Webb et al. 2011).

Infection with influenza virus is usually self-limiting. It favors secondary bacterial infection through various mechanisms like altering the respiratory epithelium. Diabetes mellitus, pregnancy, extremes of age, immunosuppression,

Fig. 22 A 29-year-old man with H1N1 pneumonia: chest radiograph showing extensive areas of consolidation in both lungs with only a relative sparing of the left upper lung field

and underlying pulmonary or cardiac conditions are some of the factors that predispose to a fulminant infection and pneumonia, and death within 24 h may be seen in extreme cases (Oikonomou et al. 2003). Such an infection is characterized histologically by diffuse alveolar damage.

Radiological features are varied and consist of segmental areas of consolidation which may be unilateral or bilateral (Fig. 22). Pleural effusions are rare. On CT, ground-glass opacities, centrilobular tree-in-bud nodules, and patchy consolidations may be seen (Oikonomou et al. 2003).

2.5.2 Respiratory Syncytial Virus

It is an RNA virus belonging to *Paramyxoviridae* family. Almost all infants are infected with RSV by 2 years of age (Drysdale et al. 2016). RSV typically causes upper respiratory tract infections, otitis media, bronchiolitis, asthma-/viral-induced wheezing, and pneumonia. Bronchiolitis may be seen in up to 80 % of the cases (Drysdale et al. 2016). In immunocompromised individuals, it can cause severe pneumonia with high mortality (Mayer et al. 2014).

In addition to bronchial wall thickening and peribronchial nodules, typical features of RSV infection on radiography are air-trapping and hyperinflation due to bronchiolitis (Müller et al. 2007). CT reflects the features of bronchopneumonia and bronchiolitis. Multifocal consolidations/GGO with tree-in-bud nodules may be seen interspersed with areas of air-trapping (Mayer et al. 2014).

2.5.3 Measles

It is a febrile illness with rash caused by an RNA virus belonging to *Paramyxoviridae* family. It spreads from one person to another through droplet spread. The clinical manifestations are more severe in adults and immunocompromised hosts.

Bronchial wall thickening, centrilobular nodules, GGO, and interlobular septal thickening are seen on CT, and the features are nonspecific (Franquet 2011).

2.5.4 SARS-Coronavirus

Coronaviruses, commonly implicated in cold, are RNA viruses of *Coronaviridae*. In 2002, a new strain caused an outbreak in China which spread rapidly throughout the world (Peiris et al. 2003). This was called SARS-coronavirus (severe acute respiratory syndrome). Transmission occurs through droplet spread; incubation period varies from 2 to 14 days (Peiris et al. 2003).

Typical symptoms are fever with myalgia and cough. Characteristic early CT findings include focal ground-glass opacities and crazy-paving pattern which are scattered in distribution. Subsequent development of consolidations may be seen. Air leak syndromes with development of spontaneous mediastinum or pneumothorax have also been reported. Residual fibrosis and scarring may also be seen (Chan et al. 2004).

2.5.5 Hantavirus

Hantaviruses are a group of RNA viruses belonging to the family *Bunyaviridae* (Mattar et al. 2015). Unlike other infections of *Bunyaviridae*, infection with hantaviruses is a rodent-borne zoonosis that spreads through inhalation of rodent secretions (feces, urine, or saliva), and humans are accidental hosts (Manigold and Vial 2014). Each species of hantavirus is associated with a unique rodent host, and thus the epidemiology of hantavirus infections correlates closely

with the geographical distribution of the respective rodents (Manigold and Vial 2014).

Infection with hantaviruses causes two distinct clinical pictures: hemorrhagic fever with renal syndrome (HFRS) which is more common in Europe and Asia, caused by the "old world" hantaviruses, and hantavirus cardiopulmonary syndrome (HCPS) which is more common in the Americas, caused by the "new world" hantaviruses (Mattar et al. 2015; Manigold and Vial 2014). Close to 150,000–200,000 cases occur every year, commonly in Asia (Manigold and Vial 2014). In Germany, a peak in 2012 with more than 2800 new cases was reported (Kruger et al. 2013).

Pathologically both these infections are characterized by breakdown of the endothelial barrier in blood vessels and marked vasodilatation.

HFRS is characterized by fever followed by hypotension and petechial hemorrhages due to vascular leakage, oliguric phase, polyuric phase, and convalescence. Oliguric phase is the most critical phase characterized by renal failure and pulmonary edema, and most of the case fatalities occur in this stage.

After an incubation period of 9–35 days, HCPS is characterized by abrupt onset of fever and other constitutional symptoms. In the next cardiopulmonary phase, cough, dyspnea, tachycardia, and hypotension occur due to extravasation of fluids as a result of increased capillary leakage. Rapidly progressive noncardiogenic pulmonary edema and cardiogenic shock may be seen with respiratory failure and need for ventilator support. Case fatality rate is high (Manigold and Vial 2014).

Chest radiography shows features of permeability edema: in mild cases, pleural effusions and interstitial infiltrates are seen (Fig. 23). In severe cases, marked alveolar edema with predominance in the perihilar and basal regions and sparing of the periphery is typical (Boroja et al. 2002). CT shows extensive GGO in middle and lower zones with thickening of the septa (Gasparetto et al. 2007).

2.5.6 Adenovirus

They are DNA viruses belonging to *Adenoviridae* family. Many serotypes exist.

Fig. 23 A 32-year-old man with hantavirus infection: CT showing extensive thickening of the septa, areas of ground-glass, and minor pleural effusions

Adenovirus is a common cause of upper respiratory tract infection in children. Severe infection is seen in immunocompromised patients. It causes sequelae such as bronchiectasis, obliterative bronchiolitis, and Swyer-James syndrome (unilateral hyperlucent lung).

Pathologically, severe adenovirus pneumonia is characterized by areas of hemorrhagic consolidation, interspersed with air-trapping, atelectasis, and diffuse alveolar damage (Becroft 1967). In mild cases, inflammatory cell infiltrate in the alveoli and interstitium is seen (Chong et al. 2006).

Radiographs show unilateral or bilateral parenchymal opacities. Especially in children, areas of overinflation and atelectasis may be seen (Kim et al. 2002). On CT, extensive GGO with or without consolidations are noted. GGO correlates with areas of diffuse alveolar damage. In a study by Chong et al. in five adults with adenovirus pneumonia, one patient had shown crazy-paving appearance (Chong et al. 2006).

2.5.7 Herpes Simplex Type 1

Herpes simplex type 1 is a DNA virus of the *Herpesviridae*, along with CMV and varicella zoster virus. Primary infection is usually asymptomatic, but can manifest as pharyngitis or

gingivostomatitis. Following initial infection, it remains latent and can undergo reactivation at a later stage and manifest as esophagitis or tracheobronchitis.

Pneumonia due to HSV-1 occurs commonly due to contiguous spread from upper respiratory tract or aspiration and less commonly due to hematogenous spread (Graham and Snell 1983; Ramsey et al. 1982). HSV-1 pneumonia is almost exclusively seen in immunosuppressed individuals or in patients with squamous metaplasia of the airways due to intubation, burns, or chronic smoking (Ramsey et al. 1982).

Fever, dyspnea, chest pain, and productive cough are usual clinical features. Herpes labialis and extensive oropharyngeal lesions may also be seen (Simoons-Smit et al. 2006).

The epithelial lesions are characterized by ulceration and necrosis. Pneumonia shows alveolar necrosis and exudate with inflammation (Kim et al. 2002).

On radiography, patchy segmental or lobar consolidation is usually seen, and pleural effusions are common (Aquino et al. 1998). On CT multifocal areas of GGO and consolidation are seen (Kim et al. 2002).

2.5.8 Cytomegalovirus

Cytomegalovirus (CMV) is a member of herpes family and is a DNA virus. It is well known to cause opportunistic infections in immunosuppressed individuals especially in bone marrow or solid organ transplant recipients and AIDS patients.

Clinical features include fever, cough, and dyspnea.

The pathological features of CMV infection in transplant recipients are reported to be different from those seen in AIDS patients. In transplant recipients, predominant necrotizing pneumonia is seen due to immune-mediated mechanisms, and CMV pneumonia is seen in the first few months after transplantation. AIDS patients, on the other hand, have insufficient immune response and show effects primarily due to the cytopathic effect of the virus with diffuse alveolar damage (Kim et al. 2002).

Radiographic manifestations are nonspecific and consist of reticulonodular pattern and/or airspace consolidations. CT features consist of diffuse or focal ground-glass opacities (GGO), multiple nodules, and lobar consolidation. Nodular lesions with surrounding GGO (halo sign) may be occasionally seen, GGO representing hemorrhage or inflammation (Franquet et al. 2003). Dense consolidation or mass-like opacities may be seen in AIDS patients especially with Kaposi's sarcoma (McGuinness et al. 1994).

2.5.9 Varicella Zoster

Varicella zoster is another virus belonging to *Herpesviridae* group. It causes two major manifestations: chickenpox (varicella) and herpes zoster. Pneumonia occurs most commonly in patients with chicken pox, although it may be seen in both forms (Müller et al. 2007).

Chickenpox is usually seen in children 2–8 years old; however, in recent times, the incidence in adults is increasing due to various factors (Mohsen and McKendrick 2003). While the common varicella infection in children is usually benign, infection in adults has a more fulminant course with a 25 times increased risk of pneumonia and consequent high mortality (Mohsen and McKendrick 2003).

Predisposing factors for the development of varicella pneumonia are immunosuppression, chronic lung diseases, pregnancy, or underlying malignancy like leukemia or lymphoma (Müller et al. 2007). Varicella pneumonia presents about 1–6 days after the onset of rash with cough, dyspnea, fever, and sometimes chest pain and hemoptysis (Mohsen and McKendrick 2003).

The pulmonary lesions in varicella seem to be due to hematogenous spread rather than airborne entry. The lesions are characterized by endothelial damage in pulmonary vessels with focal hemorrhagic necrosis, mononuclear infiltrates in the alveolar walls, and exudates in the alveoli (Mohsen and McKendrick 2003). Later small nodules are seen which are characterized by outer lamellated fibrous capsule and inner necrotic or hyalinized collagen with varying degrees of calcification (Kim et al. 1999).

On radiographs multiple, fleeting 5–10 mm miliary nodules are seen with a tendency to coalesce (Fig. 24). These resolve usually in a
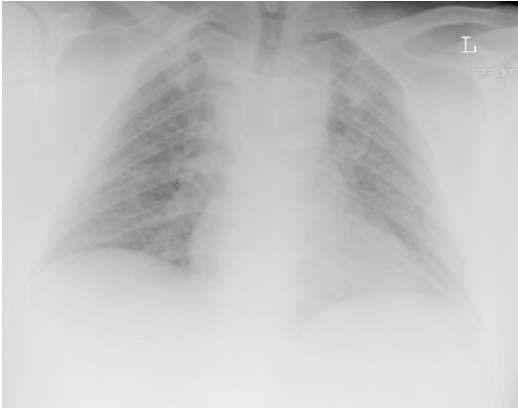
Fig. 24 A 35-year-old man with varicella virus infection: chest radiograph showing multiple fleeting 5–10 mm miliary nodules in both lungs
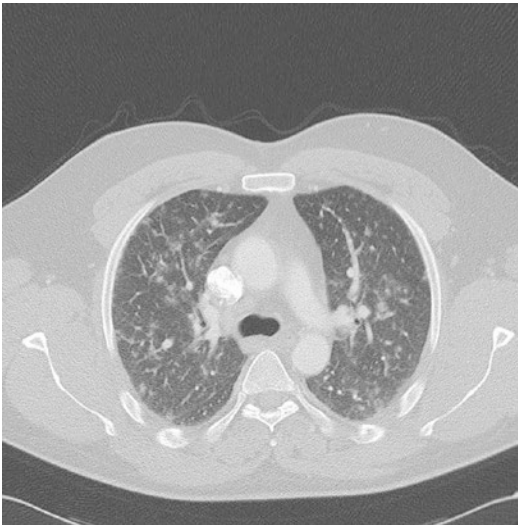

Fig. 25 Same patient as in Fig. 24: CT showing bilateral 5–10 mm nodules of soft tissue density and a ground-glass halo

week after the regression of the skin lesions, but may also be persistent for months in some patients (Sargent et al. 1966). On CT bilateral nodules of soft tissue density measuring 5–10 mm are seen (Fig. 25). Some nodules show GGO around them, while some may coalesce with adjacent nodules (Kim et al. 1999). Hilar lymph nodes and pleural effusions are less commonly seen. Dense, calcified random dense nodules measuring 2–3 mm in size may persist in some cases.

2.6 Conclusion

Although radiography and CT can be helpful in excluding a CAP, they may not be accurate in suggesting an etiological diagnosis. In every case, careful attention to the clinical history and radiological findings may help to narrow down the etiology and suggest the diagnosis.

3 Tuberculosis

3.1 Introduction

Tuberculosis is often a challenge to the clinicians and radiologists alike, particularly in areas where it is not endemic. As the clinical signs and symptoms are often nonspecific, extra attention and a high degree of suspicion are required to make the right diagnosis.

As the manifestations of tuberculosis are a result of the interaction between the offending bacteria and the host immune system, there is no definite radiological picture that defines or is typical for tuberculosis and a wide range of differential diagnoses exist. However, some features, particularly when seen in typical distributions and typical combinations, can be very helpful in suggesting the right diagnosis, as discussed below.

3.2 Background

Tuberculosis (TB) or *captain of all these men of death* is one of the oldest diseases known to mankind. It is still a disease of global concern, affecting millions of people worldwide every year. It is a leading cause of death among infectious diseases. Together with HIV, TB accounted for a staggering 1.5 million deaths in 2014 (World Health Organization 2015). Ninety-five percent of these deaths were reported in low- to middle-income countries, where tuberculosis is highly prevalent (World Health Organization 2015).

Although the incidence of TB globally has been showing a declining trend for several years, still an estimated 9.6 million new cases were

reported by WHO in 2014. Majority of these cases were reported in Southeast Asia, Western Pacific, and Africa with highest number of incident cases seen in India, Indonesia, and Nigeria. 12 % of these patients were HIV positive, and notably 75 % of HIV-positive people with tuberculosis lived in Africa (World Health Organization 2015).

Europe accounts for 4 % of TB burden in the world with close to 1000 new cases per day (European Centre for Disease Prevention and Control 2015). Within the EU/EEA (European Union/European economic area), an overall declining trend in TB reporting in the last 10 years has been observed. It is noteworthy that a significant 28 % of cases were of foreign origin. In some countries like Luxemburg, Malta, Norway, Sweden, and Switzerland, the TB cases of foreign origin accounted for >70 % cases, highlighting the increased prevalence in migrants, with an increased prevalence of MDR-TB in these groups of patients (European Centre for Disease Prevention and Control 2015; Odone et al. 2015).

The early diagnosis and treatment are further challenged by the development of multidrug-resistant and extensively drug-resistant tuberculosis. Multidrug-resistant tuberculosis (MDR-TB) is defined by resistance to the two most powerful first-line drugs, isoniazid and rifampin. WHO reported that in 2014, around 3.3 % of new cases and 20 % of previously treated cases had MDR-TB. Extensively drug-resistant tuberculosis (XDR-TB) is defined as MDR-TB with additional resistance to at least one fluoroquinolone and one of the second-line injectable drugs (World Health Organization 2015). It is estimated that around 9.7 % people with MDR-TB have XDR-TB (World Health Organization 2015).

These large numbers of TB prevalence and drug resistance signify the importance of early diagnosis and treatment. To understand imaging features in tuberculosis, an understanding of the epidemiology and pathophysiology is an important prerequisite so that a high index of suspicion in appropriate clinical settings can favor a timely diagnosis, avoid life-threatening complications, and prevent further spread of this dangerous disease.

3.3 Etiology

TB is caused by bacteria of the group *Mycobacterium tuberculosis* complex. It comprises of various bacteria; common ones causing infection in humans are *Mycobacterium tuberculosis and M. bovis. M. tuberculosis* accounts for the majority of tuberculosis cases, whereas *M. bovis* is less commonly implicated due to routine pasteurization of milk.

M. tuberculosis is an obligate aerobic, nonsporing, nonmotile bacillus. Its cell wall is rich in mycolic acid, accounting for its staining properties. It resists staining by the usual Gram method, being neither Gram negative or positive. When stained with dyes such as Ziehl-Neelsen, it resists decolorization by the acid alcohol and is therefore called acid fast. It is a facultative intracellular parasite, which preferentially resides in the human macrophages. Many of these properties explain its pathogenicity and virulence.

3.3.1 Transmission

Person-to-person transmission of infection occurs through inhalation of droplet nuclei which are expelled/discharged into the air when a patient with active pulmonary or laryngeal TB coughs, talks, or sings (Leung 1999). Patients with cavitation in the lungs, sputum culture-positive TB, and sputum smear-positive pulmonary TB who expectorate around 10^6–10^7 acid fast bacillus (AFB) per mL of sputum are more contagious than sputum-negative patients (as they expectorate usually less than 10^3 AFB per ml) (Sepkowitz 1996). Additional factors that favor the spread are an improper ventilation which promotes prolonged suspension of the droplet nuclei, crowded living conditions, and prolonged contact with an "open" case.

Open tuberculosis: Not all patients with pulmonary tuberculosis are infectious to others. Those patients who show sputum positivity for the acid fast bacilli are notably more contagious than sputum-negative cases (see above). The presence of cavitation and evidence of endobronchial spread (tree-in-bud) on radiological examination serves as an indication that there is a communication between the lung lesions and

the airways, thereby increasing the risk of infectivity. These "open" cases must be isolated from others.

3.4 Pathogenesis, Clinical, and Radiological Features

Classical teaching explains the lesions of pulmonary tuberculosis based on the time since infection. It states that primary disease after a recent infection manifests itself in lower lobes, lymph nodes, or as pleural effusion, whereas reactivation of latent tuberculosis causes an upper lobe predominant disease with cavitation. Although this classical "dogma" of tuberculosis which classifies the lesions based on the time since infection is widely accepted since time immemorial, it has been challenged in the recent past (Rozenshtein et al. 2015).

Recent studies based on molecular epidemiology using restriction fragment length polymorphism suggest that radiological features of pulmonary tuberculosis do not depend on time since infection (Jones et al. 1997; Glynn et al. 1999). Rather, the lesion manifestations depend on the immune status of the host. Infected persons who are immunocompetent develop apical disease with cavitation. Patients who are immunodeficient, on the other hand, develop lower lobe predominant disease with consolidation and lymphadenopathy without evidence of cavitation. This group includes HIV-positive adults with low CD4 counts and also children, as their cellular immunity is relatively weak.

This concept is further supported by the fact that HIV-positive patients with TB who have CD4 counts >200/mm^3 are more likely to develop apical predominant disease with cavitation (positive predictive value >78 %) and those patients with CD4 cell counts <200/mm^3 are more likely to have a predominantly lower lobe disease (positive predictive value 84 %), irrespective of the time since infection (Post et al. 1995).

Further studies in the coming future can make this distinction clear. Though the ongoing debate about the pathophysiology of TB has been discussed above, the terms from classical teaching, i.e., primary and reactivation tuberculosis, will be used here for the sake of simplicity as most of the literature is based on this terminology.

3.4.1 Pathogenesis

Primary Tuberculosis
Tuberculosis in a previously unexposed individual is described as primary tuberculosis. Once inhaled, the bacilli traverse the upper airways and reach the alveoli where they are phagocytosed by the pulmonary macrophages.

The subsequent outcome of infection depends on the interaction between the microbicidal capacity of the macrophage and the virulence of *Mycobacterium tuberculosis* bacillus (MTB). If the MTB are destroyed at this stage, no disease develops. But if the macrophage is not able to contain the infection or the bacillus is highly virulent, MTB multiplies multifold before the macrophage bursts. Release of various cytokines by the macrophages attracts further macrophages which phagocytose the released MTB (Knechel 2009). In the first 2–3 weeks, development of T cell-mediated immunity causes activation of macrophages which then destroy the MTB within them (van Crevel et al. 2002). This causes the formation of a typical granuloma with a caseation necrosis in the lungs and the draining lymph nodes. This attributes to the typical imaging features in primary TB. Thus, in tuberculosis destruction of the host tissue occurs as a part of the host immune response.

Once the infection is successfully brought under control, the patient becomes asymptomatic, although MTB may still lie inactive within the macrophages. Healing of the lesions occurs with fibrosis, and dystrophic calcification may also be seen (Pratt 1979).

In immunosuppressed hosts, extensive hematogenous spread of infection can manifest as a miliary TB, with multi-organ involvement.

Reactivation/*Post*primary TB
Many years, typically 3–5 years later, commonly due to reactivation and less commonly due to reinfection, there is a resurgence of the disease (Leung 1999). This stage, in previously sensitized individuals, is known as postprimary TB.

The disease is typically seen in apical and posterior segments of the upper lobes and apical segments of the lower lobes, probably due high oxygen tension and impaired lymphatic drainage in these areas which favor the growth of this obligate aerobe (Leung 1999). As the infection proceeds, the area of necrosis increases in this area, under liquefaction, and then decompresses itself into an adjacent bronchus. As a result of the formation of this communication with airways, air enters the lung parenchyma in this area of consolidation, forming what is a typical lesion of the secondary TB, that is, a cavity. As the contents of the cavity are discharged into the bronchus, the patient develops cough with expectoration. Spread of these discharges into the airways may also give rise to typical imaging appearance of endobronchial spread. When there is no cavity, endobronchial spread of Tb may still be seen due to endobronchial rupture of a lymph node, hematogenous spread of infection (Leung 1999).

3.4.2 Clinical Features

Majority of the TB cases are pulmonary with around 1/3 cases being extrapulmonary.

The clinical symptoms of tuberculosis are to an extent dependent on patient's age and immune status. At extremes of age, in children and elderly, the symptoms tend to be nonspecific and cause a delay in the diagnosis. Primary TB is most commonly seen in children, particularly in endemic areas. However, it is increasingly being seen in adults too.

The usual symptoms in pulmonary TB are cough with expectoration, low-grade fever with evening rise of temperature, malaise, and loss of weight (American Thoracic Society 1990). Hemoptysis and chest pain may also be seen.

Radiological Features

Primary pulmonary tuberculosis manifests itself radiologically variably as parenchymal opacities, lymphadenopathy, and/or pleural effusion. Chest radiography is usually the first imaging modality to suspect primary TB; however, the lesions are better appreciated on CT.

The granulomatous lesion in the pulmonary parenchyma is seen radiologically as an area of consolidation. It tends to be unilateral, in the

Fig. 26 A 7-year-old boy with primary TB: chest radiograph showing enlarged left hilar shadow

middle or lower lobe, and is commonly observed on the right side (Leung et al. 1992). Multifocal involvement may also be seen in 12–24 % (Woodring et al. 1986). It is usually homogenous and dense, segmental, or lobar in distribution. The lesion can also be nodular or linear in appearance.

In two-thirds of the cases, the consolidation resolves without any sequelae (Leung 1999). In the remaining one-third cases, it heals with the formation of a linear scar or fibrosis, with calcification. This focus is called as Ghon's focus (Leung 1999). Tuberculomas which are mass-like opacities and satellite calcifications may be also seen in 9 % of the cases.

Lymphadenopathy is the most characteristic feature of primary TB. It is seen in 90–95 % of the children with primary TB. As the age increases, the prevalence of lymphadenopathy decreases in older children and adults (Leung et al. 1992). Tuberculous lymphadenopathy tends to be typically unilateral with frequent involvement of the right paratracheal and right hilar groups. This can be visualized on radiographs with the widening of the right paratracheal stripe and enlarged hilum, respectively (Fig. 26). On CT, the presence of enlarged lymph nodes, more than 2 cm with peripheral rim enhancement, is characteristic (Fig. 27). This is due to central caseous necrosis with peripheral vascular granulation tissue (Leung et al. 1992).

Fig. 27 A 7-year-old boy with primary TB: axial CT thorax in the same patient with mediastinal window showing enlarged left hilar lymph nodes with peripheral contrast enhancement

Fig. 28 A 27-year-old patient with reactivation tuberculosis: axial CT showing a thin-walled cavitary lesion in the posterior segment of the right upper lobe. Florid areas of centrilobular nodules with tree-in-bud appearance are noted on both sides. This combination is highly suggestive of reactive tuberculosis

The enlarged lymph nodes can cause extrinsic compression of the airways. Complete obstruction of the lumen manifests as segmental or lobar collapse of the distal lung (Andreu et al. 2004). Partial obstruction, on the other hand, can present with air-trapping and hyperinflation of the involved lobe due to ball-valve-like effect and subsequent trapping of air (Arora et al. 2013).

Healing of the granulomatous lesions with dystrophic calcification leads to the formation of calcified hilar lymph node with a calcified pulmonary Ghon's lesion, also known as Ranke's complex. It serves as a telltale sign of previous TB infection in the past.

Reactivation tuberculosis is characterized by parenchymal opacifications, predominantly in the posterior and apical segments of upper lobes and apical segment of lower lobes. Multisegmental involvement is often seen. Atypical distribution involving *exclusively* other segments is rare and is seen in approximately 5% of the cases of postprimary TB (Woodring et al. 1986). Cavities are seen in 40–45% of cases of postprimary disease. They may be single or multiple and have varied appearances ranging from thick walled to thin walled. Cavities usually occur in areas of consolidation. Cavities may mimic carcinoma; however, careful attention to adjacent bronchogenic spread with tree-in-bud lesions and satellite nodules may aid in the diagnosis.

When an area of caseous necrosis erodes into adjacent airways, bronchogenic spread is seen. It is an important hallmark of the activity of the disease. CT is more sensitive in demonstrating bronchogenic spread: in one study by Im et al., bronchogenic spread was notably seen in 95% of patients with postprimary TB, while radiography showed these findings reliably only in 20% patients (Im et al. 1993). Earliest markers of bronchogenic spread are sharp centrilobular nodules or linear branching opacities 2–4 mm in diameter. In extensive bronchogenic spread, a typical tree-in-bud appearance is described, the stalk represents the distal airways, and the bud represents alveolar ducts and bronchioles, which are filled with caseous material. Other signs of bronchogenic spread are bronchial wall thickening with or without bronchiectasis, poorly defined nodules 5–8 mm in diameter. Interlobular septal thickening may also be seen. These changes signify an active underlying disease and regress with effective treatment in 5–9 months (Im et al. 1993).

Tree-in-bud nodules are not specific for tuberculosis. However, presence of cavitary or nodular lesions in the typical distribution along with tree-in-bud lesions makes the diagnosis of tuberculosis highly probable and should always be considered in suitable clinical settings (Fig. 28) (Andreu et al. 2004).

Complete regression of the parenchymal lesions may be seen when healing occurs before the development of caseous necrosis, which is however rare (Pratt 1979). In posttreatment changes with development of distortion of bronchovascular structure, fibrotic bands in areas of caseous necrosis are well established. Areas of paracicatricial emphysema may develop due to bronchostenosis and traction (Im et al. 1993). Marked fibrotic reaction with upward hilar retraction is typical and may be seen in one-third of the cases. Apical pleural thickening, usually less than 1 cm, may also be occasionally seen (Woodring et al. 1986).

When to Think of TB?

Patient features: Migratory background, poor immune status

Radiological features: Primary TB: Unilateral dense segmental or lobar consolidation in lower or middle lobes, lymphadenopathy with central hypodensity on CECT

Reactivation TB: Cavitation in apical segments, centrilobular tree-in-bud nodules, with or without sequelae of primary TB infection

---

Hilar and mediastinal lymphadenopathy is less likely in postprimary tuberculosis. Spontaneous pneumothorax may be seen in extensive cavitary disease, although rare.

Miliary TB

At any stage, either after primary or postprimary, a fulminant infection can give rise to disseminated infection with multiple granulomas seen in various organs. These granulomas resemble millet seeds, and thus the term "miliary" tuberculosis was used to describe them. Various conditions that predispose to the development of miliary TB are HIV/AIDS, malnutrition, diabetes mellitus, underlying malignancy, immunosuppression, treatment with corticosteroids, and immunomodulators (anti-TNF alpha agents) (Sharma et al. 2012).
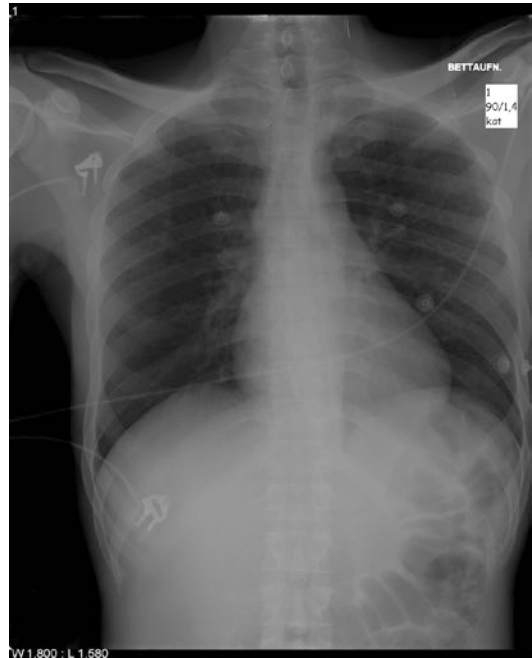

Fig. 29 A 52-year-old HIV-positive male with miliary tuberculosis: frontal radiograph showing multiple vague nodular lesions in both the lungs

Early radiographs may be normal. Evenly distributed nodules roughly 1–3 mm in size may be seen (Fig. 29). CT demonstrates these changes more clearly with sharply and poorly defined nodules seen in random distribution with respect to the secondary pulmonary lobule (Figs. 30 and 31). Smooth thickening of the interlobular septa is commonly seen (McGuinness et al. 1992). Ground-glass opacities may be seen for abnormalities that are below the resolution of CT (Hong et al. 1998). On adequate treatment, these nodules resolve usually without any residual fibrosis.

In some cases, military tuberculosis can progress to adult respiratory distress syndrome. Spontaneous pneumothorax due to rupture of subpleural nodules has also been reported (Sharma and Kumar 2002).

3.5 Pleural Involvement

Pleural effusion can be seen not only as a part of primary TB but also in patients with reactivation TB and is thus not specific for any stage of TB.
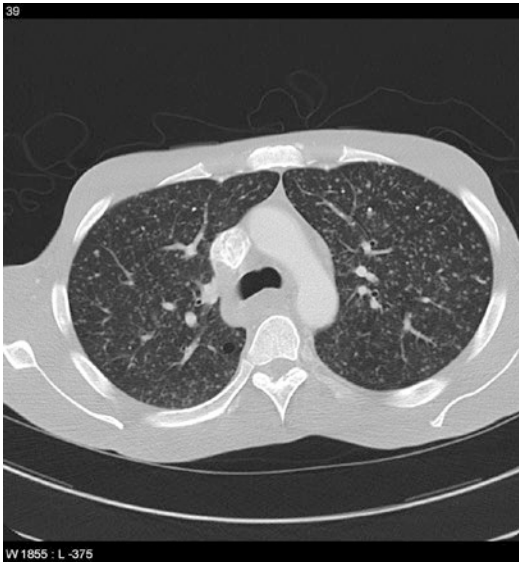
Fig. 30 A 52-year-old HIV-positive male with miliary tuberculosis: axial CT showing multiple well-defined nodules in a random distribution much better

Fig. 31 A 52-year-old HIV-positive male with miliary tuberculosis: axial MiP image showing multiple miliary nodules in a random distribution better

It occurs supposedly due to a delayed hypersensitivity reaction as a result of rupture of a caseating subpleural focus into the pleural cavity. The release of inflammatory mediators causes accumulation fluid in the pleural space, which is an exudate.

Tuberculous pleuritis often presents acutely with rapid onset of pleuritic chest pain that is worsened by deep breathing, fever, and cough. In HIV-positive patients, a more subacute course is

described. It is usually unilateral, often seen on the same side of the parenchymal lesion. Isolated pleural effusions without any parenchymal lesion are not rare.

On ultrasound examination, it often shows septations which are usually not appreciated on CT (Cardinale et al. 2015). On contrast-enhanced CT, pleural fluid of fluid density with smooth peripheral pleural enhancement, "split pleura" is typical (Yilmaz et al. 1998). Presence of a changing air-fluid level in the pleural space mandates ruling out a bronchopleural fistula (Johnson et al. 1973).

3.6 Airway Involvement

The involvement of airways in tuberculosis is seen in 10–20% of patients with pulmonary tuberculosis (Moon et al. 1997). Various mechanisms responsible for the involvement of airways are spread of infection from the parenchymal lesion along the peribronchial lymphatic channels, implantation from infected sputum, erosion of an adjacent lymph node, or hematogenous spread (Moon et al. 1997; Kim et al. 1997).

Acute tracheobronchitis with involvement of the distal trachea and the proximal bronchi may be seen (Kim et al. 1997). Tracheobronchial TB is characterized commonly by a long-segment thickening (>3 cm) (smooth or irregular), causing circumferential narrowing of the airways. Less common appearances are that of a granulomatous, polypoid ulcerated mass (Andreu et al. 2004).

Chronic inflammation of the airways may cause tracheal or bronchial stenosis. Traction bronchiectasis due to fibrosis is often seen as sequel of infection.

A calcified peribronchial node that usually erodes into the adjacent bronchus is a common cause of broncholithiasis. Common sites are the proximal right middle lobar bronchus and anterior segmental bronchus of the right upper lobe.

3.7 Pericardial Involvement

Tuberculous pericarditis is seen in around 1% pulmonary TB patients; the incidence is rising

due to HIV-TB coinfection (Mayosi et al. 2005). In HIV-infected groups, 85 % of the cases of pericardial effusion are due to TB (Ntsekhe and Hakim 2005). It may present as pericardial effusion, constrictive pericarditis, or a combination of both.

The spread of infection to the pericardium occurs chiefly through the following routes:

Via infected mediastinal lymph nodes: predominant in immunocompetent individuals, it is largely a hypersensitivity reaction with paucibacillary status.

Via hematogenous route: more often encountered in HIV-positive and other immunosuppressed individuals, where is it often a more florid infection with a multibacillary status (Ntsekhe and Mayosi 2013).

Less common mode of spread is via direct spread from an adjoining pulmonary infection.

Clinical Features Typically, an insidious onset, with complaints of fever, dyspnea, chest pain, and malaise, is described. Cardiac tamponade may be frequently seen and is a late feature. Acute presentation with dyspnea, fever, and retrosternal chest pain is also possible.

Imaging On routine chest radiography, enlarged cardiac silhouette is seen in tuberculous effusion. Concomitant evidence of active pulmonary tuberculosis may be seen in 30 % of the individuals, and 30–50 % may show pleural effusions (Reuter et al. 2005). Another interesting feature to note is that the hilar lymph nodes are not usually involved; mediastinal nodes not detected with PA radiographs and therefore the lymphadenopathy in tuberculous pericarditis are not seen on routine frontal radiographs (Reuter et al. 2005). On echocardiography, pericardial thickening with evidence of strands in the fluid is commonly seen in around 60 % cases and is not specific for TB pericarditis (Mayosi et al. 2005).

Imaging features on CT may point to the tuberculous origin of the effusion. Thickened enhancing pericardium is seen; however, it may be difficult to distinguish between small effusions and thickening on CT, where ultrasound may prove more helpful. In one study, enlarged

mediastinal lymph nodes were described in all patients with tuberculous pericarditis (Cherian 2004). These lymph nodes usually regress with treatment. On the contrary, other causes of effusion with mediastinal lymphadenopathy, like lymphoma, malignancy, or sarcoidosis, show hilar lymphadenopathy in addition

In constrictive pericarditis, fibrous or calcific thickening of the pericardium is seen, with or without effusion. Pericardial thickening of more than 3 mm with supporting findings of dilated inferior vena cava and deviated interventricular septum can help in accurate diagnosis, in appropriate clinical settings. Calcification of the visceral pericardium in the atrioventricular groove, interventricular groove, and crux of the heart is uncommon but may be seen (Suchet and Horwitz 1992).

3.8 Acute Complications: Tuberculosis in the Emergency Room

Tuberculosis, although as described above, has an insidious onset and progress, can also present acutely, in a previously healthy person. Common symptoms with which the patients present to the emergency room are dyspnea, fever, hemoptysis, or chest pain. It may be a challenge to diagnose tuberculosis in acute settings, especially in countries where it is less endemic and a wide other close differential diagnoses exist. However, an awareness of the migratory background and immune and HIV status of the patient, compounded by a high index of suspicion of the treating physician and the radiologist, may expedite the diagnostic process.

3.8.1 Hemoptysis

Hemoptysis, or expectoration of blood, is an acute life-threatening complication of tuberculosis. Incidence of hemoptysis in TB may be up to 7 %, depending upon the regional prevalence of tuberculosis, with a high mortality rate ranging from 9 to 18 % (Krishnan et al. 2009; Johnston and Reisz 1989; Alkhuja and Miller 2001). Hemoptysis in TB does not always signify an underlying active disease (Prasad et al. 2009).

Massive hemoptysis is defined variably in the literature, with the volume of blood ranging from 100 to 1000 mL in 24 h, although any amount of bleeding that causes hemodynamic instability should be considered significant (Corder 2003; Jean-Baptiste 2000). Almost 90 % of causes of massive hemoptysis in general originate from bronchial vessels, while 10 % originate from pulmonary vessels, understandably because the bronchial vessels are at systemic pressure (Yoon et al. 2002). Notable among the common causes are chronic inflammatory conditions like bronchiectasis, tuberculosis, and lung abscess and malignancies like bronchogenic carcinoma, which account for a vast majority of cases of massive hemoptysis.

The first step in managing any patient with massive hemoptysis is stabilization of the patient, resuscitation, and protection of the lower airways, as the risk of death due to asphyxiation overweighs that due to exsanguination (Marshall and Jackson 1997).

The next step is to identify the site and cause of bleeding and treat it accordingly. Various procedures form a part of the diagnostic algorithm for further evaluation, with MDCT angiography followed by bronchoscopy standing at the forefront. If the patient is clinically stable, the first logical step will be a MDCT angiography to locate the site of bleeding. CT has many advantages as it enables not only the identification of the site of bleeding but also facilitates the evaluation of the lungs to recognize the underlying cause of bleeding (Yoon et al. 2002).

On the other hand, patients who are not stable are taken up directly for rigid/flexible fiber-optic bronchoscopy. Many studies nevertheless recommend using CT angiography prior to bronchoscopy routinely in all patients with hemoptysis, as CT aids in a comprehensive evaluation with a better diagnosis of the cause of hemoptysis compared to bronchoscopy (Revel et al. 2002; Bruzzi et al. 2006).

Causes of Hemoptysis in Tuberculosis

Several underlying pathologies in tuberculosis can cause hemoptysis. Bronchial vessels are a more common source than pulmonary vessels and, when involved, tend to cause severe hemoptysis which is difficult to control.

Tuberculous bronchitis and bronchiectasis tend to cause bronchial arterial bleeding. Tuberculosis cavities can erode into adjacent structures, for example, into pleura and chest wall, and cause hemoptysis due to the involvement of intercostal, internal mammary, or subclavian vessels. Furthermore, colonization of preexisting cavities with fungus – aspergilloma – can also present as hemoptysis. Inflammation of pulmonary artery branches adjoining the cavities of TB, with consequent formation of "Rasmussen" aneurysm, can precipitate fatal hemoptysis. Erosion of the involved lymph nodes into adjacent tracheobronchial tree or vessels may also cause hemoptysis (Chatterjee et al. 2015; Halezeroglu and Okur 2014).

Bronchiectasis and Dilatation of Bronchial Arteries

Bronchial arteries are the primary source of nourishment to the bronchial tree and have microvascular connections with pulmonary circulation. These connections become functional in patients with bronchiectasis and chronic inflammation like TB.

In various chronic inflammatory conditions like tuberculosis and bronchiectasis (which can itself be as a result of tuberculosis), there is associated vasculitis and thrombosis of pulmonary vessels that cause local hypoxia. This stimulates the release of angiogenetic growth factors such as vascular endothelial growth factor, thereby promoting neovascularity, collateral formation, and enlarged bronchial arteries. This accounts for flow of blood from bronchial arteries at systemic pressure into the pulmonary vessels and hemoptysis (Bruzzi et al. 2006).

Special attention should be given to CT appearances in these patients. Presence of nodular or tubular soft tissue attenuation structures in the mediastinum, particularly around the airways, which are atypical for lymph nodes, should be viewed with suspicion. These structures may point toward hypertrophied bronchial arteries (Song et al. 1998).

Fig. 32 A 52-year-old patient with cavitary lesion in left upper lobe. Intracavitary body with "air-crescent" sign, suggestive of aspergilloma, is seen in the left upper lobe

Aspergilloma

Aspergilloma is a fungal infection, caused commonly due to the fungus *A. fumigatus* that saprophytically colonizes preexisting cavities, and dilated bronchi, without invading them. It is commonly asymptomatic, hemoptysis being the most common symptom. On radiography, a round or oval intracavitary mass lesion is typically described, the lesion being dependent in location and surrounded by a crescent of air (air-crescent sign). Decubitus views to demonstrate the mobility of the intracavitary mass are helpful in doubtful cases. Pathologically, the lesion comprises of fungal hyphae intermixed with varying amounts of mucous and cellular debris. On CT, a soft tissue attenuation lesion located within a cavity is typical (Fig. 32). Thickening of the walls of the cavity and that of the adjacent pleura is described. This thickening may be the earliest sign of aspergillosis, even before any visible changes in the cavity are seen. It represents a hypersensitivity reaction rather than a fibrosis and is reversible with treatment (Franquet et al. 2000).

Hemoptysis in aspergilloma is often associated with vasculitis in the cavity wall and extensive collateral formation from axillary and subclavian vessels (Uflacker et al. 1983; Remy et al. 1977). Hypertrophied bronchial arteries may also be seen as the cause of hemoptysis, and these should be actively searched for on CT.

The diagnosis can be challenging when the air crescent is not clearly appreciated due to obliteration of the cavity. Other differential diagnoses for intracavitary lesions are angioinvasive aspergillosis, echinococcal cysts, Rasmussen aneurysm in a cavity, lung abscess, bronchogenic carcinoma, intracavitary clot or hematoma, and *P. carinii* pneumonia (Franquet et al. 2001)

Treatment: Spontaneous resolution may be seen in 10 % of the patients (Hammerman et al. 1973). Palliative bronchial artery embolization is undertaken for acute management of hemoptysis, although a significantly high rate of recurrent hemoptysis in aspergillosis has been reported (Uflacker et al. 1983; Remy et al. 1977). Definitive treatment is thus surgical resection with perioperative antifungal treatment.

Rasmussen's Aneurysm

Rasmussen's aneurysm is another rare cause of life-threatening hemorrhage in tuberculosis. A prevalence of 4 % in autopsy studies in patients who died of tuberculosis has been described.

Rasmussen's aneurysm is a pseudoaneurysm which arises due to erosion of a cavity into an adjacent pulmonary artery. As the inflammation of the cavity involves an adjoining pulmonary artery branch, there is progressive weakening and thinning of the arterial wall as a result of necrotizing granulomatous inflammation, giving rise to a pseudoaneurysm months or years later (Santelli et al. 1994; Kim et al. 2001). Eventual rupture can cause fatal hemoptysis.

MDCT angiography plays an important role in not only identifying the aneurysm but also in correctly characterizing it as arising from pulmonary artery, distinguishing it from bronchial artery aneurysms which are more frequent. Careful attention to the cavity on post-contrast images may exhibit a focal enhancing lesion, thereby clinching the diagnosis.

Emergency endovascular management technique like percutaneous catheter embolization of the aneurysm is the treatment of choice (Remy et al. 1980).

Hemoptysis Due to Lymph Nodes

Although extremely rare, reports of tuberculous lymph nodes causing erosion of mediastinal

vessels like aorta or pulmonary artery with subsequent formation of trachea/bronchovascular fistula and fatal hemorrhage do exist (Krishnan et al. 2009; Fatimi et al. 2006).

3.8.2 Chest Pain/Dyspnea

Acute onset chest pain and difficulty in breathing in tuberculosis can be due to a variety of underlying causes: acute respiratory distress syndrome (ARDS), pleuritis, pneumothorax, pericarditis, chest wall abscess to name a few.

Pneumothorax: Secondary Spontaneous Pneumothorax

Pneumothorax can complicate the course of roughly 1 % of tuberculosis, more often in severe cavitary tuberculosis. Underlying pathology is rupture of pleural caseous nodules which undergo necrosis. It must be suspected when apical abnormality is seen after re-expansion of the lung (Kim et al. 2001).

Pneumothorax, which may also be bilateral, has been reported in patients with miliary tuberculosis, who present with acute onset of breathlessness during the course of treatment with antituberculous drugs (Sharma and Kumar 2002; Arya et al. 2011; Khan et al. 2011; Singh et al. 2014). Caseation of the subpleural miliary nodules with subsequent rupture into the pleural space has been attributed as the triggering factor. On imaging, miliary shadows may not be discernible initially and may be evident only when the lung re-expands.

4 Hematogenous Spread of Pulmonary Infection

4.1 Introduction

Hematogenous origin of pulmonary infection depends on septic pulmonary embolism (SPE). This is an uncommon syndrome characterized by pulmonary embolization of infected thrombi containing microorganisms admixed with fibrin. It depends on a primary infectious site spread out into the venous circulation, with implantation into peripheral pulmonary arterial vessels, resulting in alveolar infective infiltrates.

The most common causative Gram-positive bacteria are *Staphylococcus aureus* and *Streptococcus pneumoniae*, whereas the most frequent Gram-negative bacterium is *Pseudomonas aeruginosa* (Angus and van der Poll 2013).

Historically SPE was most commonly associated with Lemierre's syndrome, postpartum septic pelvic thrombophlebitis, and right-sided infective endocarditis (Mac Millan et al. 1978; Goldenberg et al. 2005).

In the last decade, attention has been made to changes in the epidemiology, including thrombophlebitis due to contiguous deep soft tissue or bone infection or for infected endovascular catheters and implantable devices (Brenes et al. 2012a; Cook et al. 2005a).

In fact, like all foreign bodies, venous catheters, cardiac pacemaker, implantable cardioverter defibrillator, and joint prosthesis could carry a risk of infection. Due to increase in the number of that devices, the risk of infections have become a common problem in clinical practice (Baddour et al. 2003).

The incidence of infections is 1.9 per 1000 devices per year, and the cumulative probability of device infections is higher among patients with defibrillators compared with those with pacemaker and central venous catheters or joint prosthesis (Uslan et al. 2007).

Approximately 25 % of acute cardiac pacemaker infections occur as an acute event, in a period of device to be installed in the first 1–2 months (Cook et al. 2005b) (Fig. 33). There is a high mortality (27–65 %) associated with infections of these devices (Klug et al. 1997).

Septic embolism also occurs in 22–50 % of patients with infective endocarditis. The predictors of embolism are vegetation size greater than 10 mm, mitral location, and infection of *S. aureus*.

The brain, the spleen, and lungs are the most frequent sites of embolism in left- and right-sided infective endocarditis (Takin et al. 2012).

4.1.1 Clinical Characteristics

Main risk factors for SPE are intravenous drug abuse, alcoholism, hemodialysis, diabetes, and venous catheters (Cassling et al. 1985) (Fig. 34).
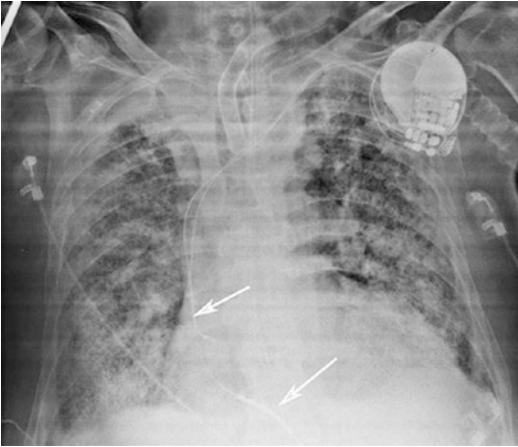
Fig. 33 Chest radiograph shows the presence of a pacemaker (*arrows*) associated with multiple lobular, patchy, pulmonary infiltrates

Fig. 34 Post-contrast CT coronary image of the mediastinum demonstrates a defect filling corresponding to a thrombus (*arrowhead*) that surrounds a central venous catheters (*arrow*) inside the lumen of superior vena cava

SPE diagnosis is based on the following criteria: acute clinical presentation with fever, chills, chest pain, dyspnea, hemoptysis, cough, presence of an extrapulmonary infectious site (such as pyelonephritis (Fig. 35) with or without hydronephrosis,

Fig. 35 Post-contrast CT axial scan of the abdomen shows multiple hypodense focal areas (*arrows*) of the right kidney, corresponding to pyelonephritis associated with a small abscess (*arrowhead*)

osteomyelitis with multiple small paraspinal abscesses, osteoarthritis (Fig. 36), liver abscesses (Fig. 37), muscle abscesses (Fig. 38), neck or oral infection (Fig. 39), etc.), frequent acute venous thrombosis that can affect any vein in the body evidenced by color Doppler-ultrasound and/or CT scan (Fig. 40), bacteremia evidenced by laboratory tests, multifocal pulmonary peripheral nodules, or infiltrates demonstrated by chest x-ray film and CT scan.

Frequently the patients with SPE have an infective endocarditis (IE) that primarily involves the cardiac valve leaflets and can spread septic emboli into the pulmonary arterial circulation. Patients with large cardiac valve-infective vegetations (>10 mm) are at high risk of pulmonary embolism. The mitral valve is the most frequent infected valve (50 %) followed by the aortic valve (40 %) and tricuspid valve (10 %). Multiple valves, usually the mitral and aortic valves, are involved in 20 % of cases (Moriera et al. 2012; Nucifora et al. 2007).

The mortality of IE is about 30–60 % and is due to septic embolism involving mitral valve, lungs, and cerebrovascular sites (Nucifora et al. 2007).

Fig. 36 Post-contrast CT axial scan of the pelvis demonstrates a thin fluid collection with air bubbles (*arrows*) inside the left hip capsule, due to osteoarthritis
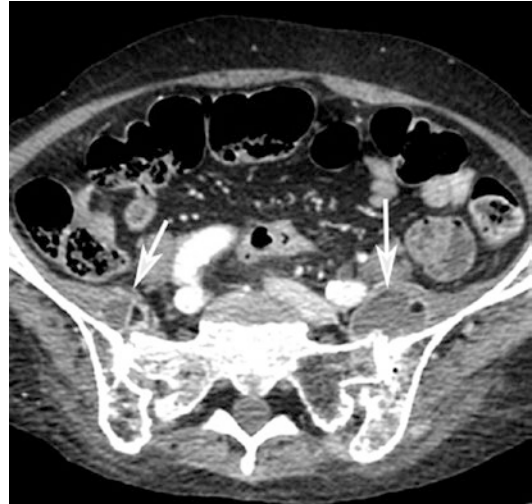

Fig. 37 Post-contrast CT axial scan of the abdomen demonstrates a large liver abscess with a typical air-fluid level (*arrow*)
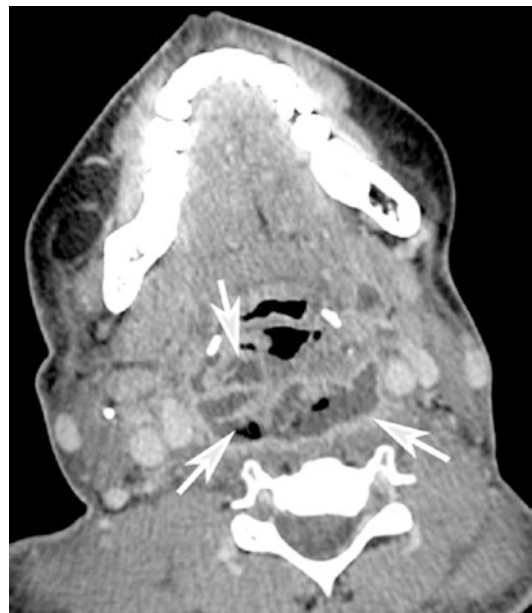

Fig. 38 Post-contrast CT axial scan of the pelvis shows bilateral iliopsoas muscle small fluid collections surrounded by a thin hyperdense capsule (*arrows*) corresponding to abscesses

Fig. 39 Post-contrast CT axial of the neck demonstrates a pharyngeal multiloculated collection surrounded by a thin hyperdense tissue (*arrows*) corresponding to abscess

4.2 Pathophysiologic Sequence

A local infection can cause extravasation of microorganisms into the venous system. Depending on the extent of the infection, edema could result in venous compression and stasis (Nourse et al. 2007) (Fig. 40).

The venous endothelium could be damaged by inflammatory mediators and production of thrombogenic toxins by the microorganism, leading to venous thrombosis. The fibrin and platelet
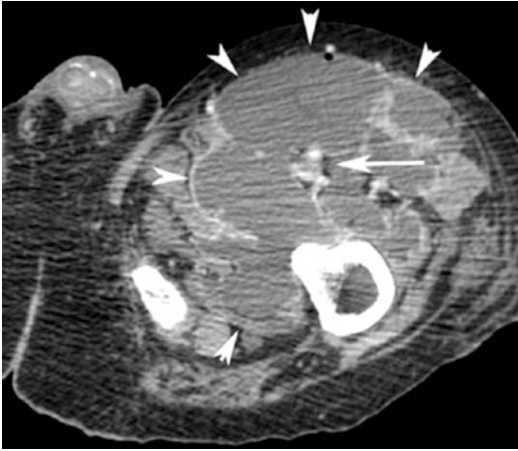
Fig. 40 Post-contrast CT axial scan of the left lower limb shows quadricipite muscle large multiloculated collection corresponding to abscess (*arrowheads*), surrounding the femoral venam that contains a thrombus (*arrow*)
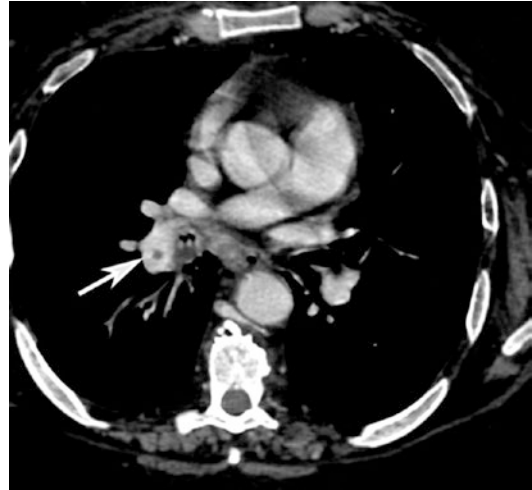

Fig. 41 Post-contrast CT axial scan of the chest shows a small defect filling corresponding to an embolus (*arrowhead*) inside the lumen of the right lower interlobar pulmonary artery

matrix serves as an ideal nidus for proliferation of the microorganism with potential for propagation and allows for distant metastatic infection as its contents are drained into the pulmonary circulation through the venous system.

Special attention should be given to *S. aureus* which can determine a severe inflammatory reaction, with direct endothelial damage through CI toxins and enzymatic mechanism, determining septic pulmonary emboli (Brenes et al. 2012b) (Fig. 41).

Specifically, it is known that *S. aureus* has a tendency to promote venous thrombosis. The bacterium produces an extracellular heat stable leukocidin that exhibits thrombogenic effects, through indirect inflammatory mechanism, including the development of reactive oxygen species and release of secondary inflammatory mediators from dying granulocytes, causing intense endothelial dysfunction (Boyle-Vavra and Daum 2007). *S. aureus* produces coagulase too, which specifically interacts with fibrinogen and causes coagulation (Gorenstem et al. 2000).

The predominance of *S. aureus* as the causative agent is related to its intrinsic thrombogenic and pro-inflammatory potential, rather than just its expected relation to the type of primary focus (Vinder Have et al. 2009; Hota et al. 2001). Once in the blood flow, the bacterium can damage

directly the pulmonary parenchyma through the toxins (Boyle-Vavra and Daum 2006) and indirectly through inflammatory mediators (Holm et al. 2011) that may occasionally promote local thrombosis which serves as an additional nidus for proliferation of the bacterium. Embolization of these thrombi, inside the pulmonary arterial circulation (Fig. 41), allows for multiple infection infiltrates of the lungs, even in the absence of heart valvular involvement.

The endothelial cells of the capillaries and arterioles as well as the venules of the lungs are highly susceptible to hypoxia. Therefore, mild transient ischemia of lung tissue may result in marked vessel dilatation as well as increased vascular permeability with fluid and erythrocyte leakage inside the alveolar sacs (Wagenwoort 1995).

4.3 Radiographic Features

Chest x-ray film is low sensitive, but can help to provide important information to suggest the diagnosis of SPE. Radiological findings are based on the evidence of multiple small diffuse lung opacities (Fig. 42), look like that of a broncopneumonia, and/or wedge-shaped opacities in the
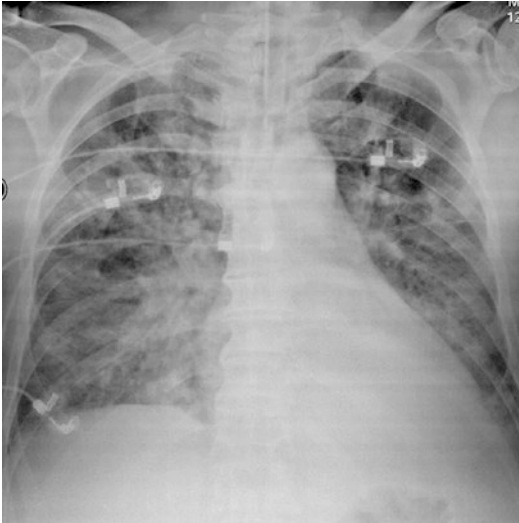
Fig. 42 Chest radiograph shows multiple bilateral lobular areas of consolidation of pulmonary parenchyma that coalescence in the right paracardiac region

Fig. 43 Chest radiograph shows peripheral pulmonary infiltrates (*arrows*) associated with pleural effusion
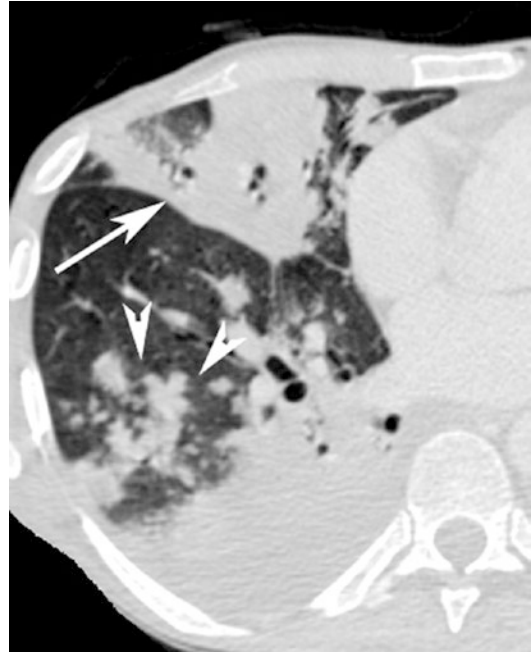

Fig. 44 CT axial scan of the chest shows a peripheral wedge-shaped opacity (*arrow*) of the medium pulmonary lobe associated with multiple patchy opacities of the lower right pulmonary lobe
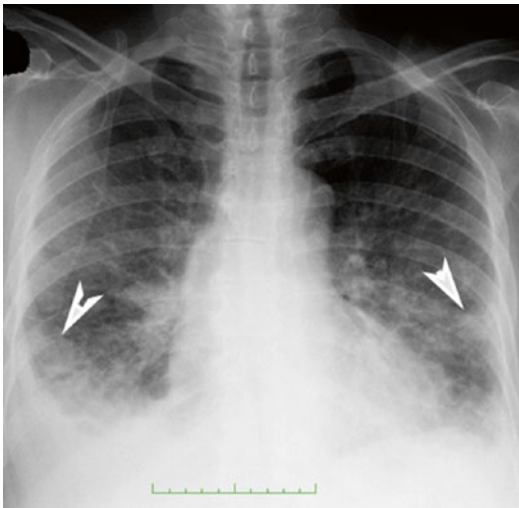
periphery of lung (Fig. 43) and nodules with or without cavitations.

The gold standard to investigate the cause of acute respiratory symptoms is chest computed tomography (Farahmand et al. 2011; Cook et al. 2005c).

The typical CT findings that indicate SPE include peripheral nodules with or without cavitations, some of them showing evidence of breakdown suggestive of septic emboli, wedge-shaped peripheral lesions abutting the pleura (Fig. 44), and patchy ground-glass opacities (Fig. 45) and feeding vessel signs (Fig. 46). Other CT findings include air bronchogram within nodules (Fig. 47), focal consolidations, lung abscesses (Fig. 48), and halo signs. About 70 % of the lesions are generally located just beneath the pleura (Fig. 49) and about feeding vessels (Fig. 50). It was reported that radiographic evidence of a nodular density suspended in a thinly walled hyperlucent cavity is characteristic of septic pulmonary emboli (Yoong and Cheong 1997; Iwasaki et al. 2001).

There is also a tendency for the septic nodules to change appearance over time. Feeding vessels are observed in nodules in 60–70 % of patients (Rossi et al. 2000; Habib et al. 2010).

The microembolism is not generally observed directly on CT scan. Indirect findings of microembolism are pulmonary edema, pulmonary infarctions, and pulmonary hypertension findings with enlargement of arterial vessels.
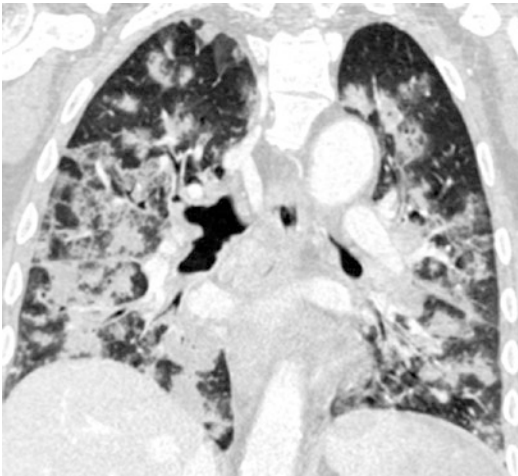
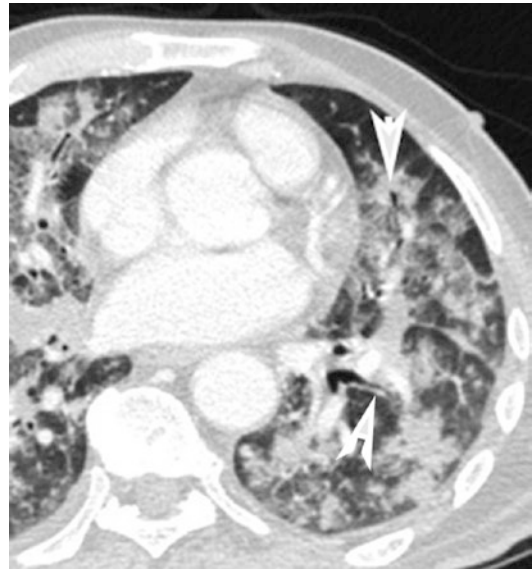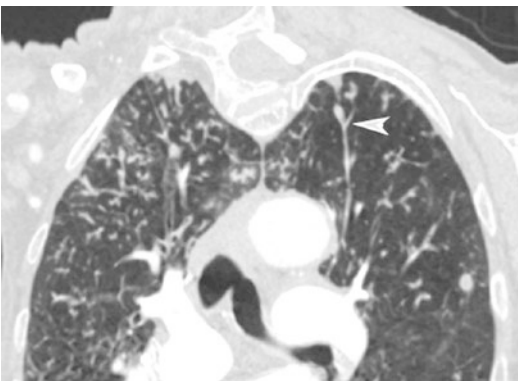**Fig. 45** CT coronal image of the chest demonstrates multiple patchy ground-glass opacities of the lungs

Fig. 46 CT coronal image of the chest demonstrates the feeding vessel sign (*arrow*)

Fig. 47 CT axial scan of the chest demonstrates air bronchogram (*arrowheads*) within patchy ground-glass pulmonary opacities
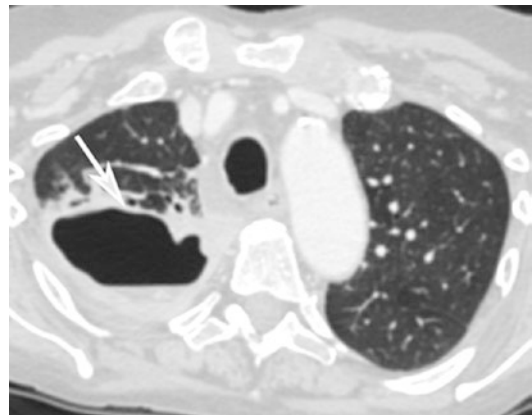

Fig. 48 CT axial scan of the chest demonstrates a large right upper pulmonary lobe abscess with a typical air-fluid level (*arrow*)

The presence of parenchymal consolidation in pulmonary infarction is mainly caused by pulmonary hemorrhage (Balakrishnan et al. 1989).

Unusual presentations of SPE include pneumomediastinum and subcutaneous emphysema (Wang et al. 2004) as well as the evidence of septic emboli in the subsegmental pulmonary arteries. Pleural effusion is also observed in 70 % of patients (Fig. 42).

The chest CT findings typically lead to cardiac imaging because of the association with right-sided infective endocarditis. The absence of obvious cardiac valvular lesions should prompt careful consideration of other potential sources of infections, including venous devices (Fig. 51), or thrombophlebitis due to soft tissue infections (Fig. 40). Additional imaging modalities including ultrasound help in delineating the root cause of infection (Gadcowski and Stout 2008).

Echocardiographic examination of all cardiac valves, including right-sided valves, should be carried out in all patients with suspecting infective endocarditis, especially when the patient has a risk factor (Chua et al. 2000). In the absence of
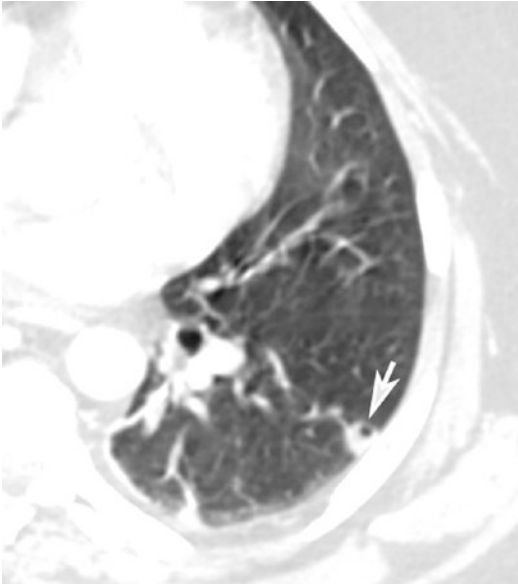
Fig. 49 CT axial scan of the chest demonstrates a small peripheral abscess with a typical air-bubble inclusion (*arrow*) localized in the left lower pulmonary lobe
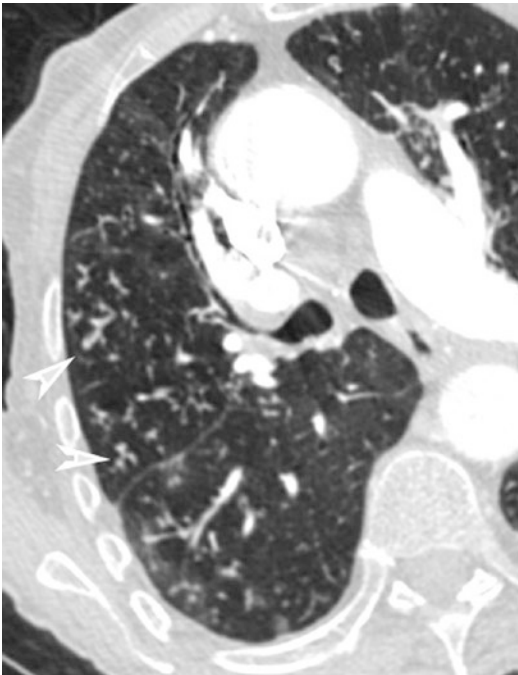

Fig. 50 CT axial scan of the chest demonstrates the feeding vessel signs (*arrowheads*)

signs of endocarditis, further evaluation to identify the infectious source is indicated (Vos et al. 2012).

Fig. 51 Post-contrast CT axial scan of the mediastinum demonstrates a defect filling corresponding to a thrombus (*arrowhead*) that surrounds a central venous catheters (*arrow*) inside the lumen of the left brachiocephalic vein

4.4 Conclusion

Sepsis is a syndrome caused by the inefficiency of the mechanism of control and containment of the infection. It is characterized by symptoms and signs of systemic inflammatory reaction to infection and manifestations of organ dysfunction, resulting from alterations in the microcirculation. It is the second common cause of death with a mortality rate between 15 and 50 % (Ferrari and Barletta 2012).

SPE has manifestations ranging from an insidious illness with fever and respiratory symptoms to acute generalized sepsis with disseminated intravascular coagulopathy or acute renal failure.

The diagnosis of SPE is based on clinical manifestations, culture data, and radiographic evidence of peripheral thrombosis and pulmonary infection. Respiratory impairment with high grade fever and marked increase of serum inflammatory markers differentiate septic pulmonary embolism from nonseptic pulmonary embolism (Melina et al. 2010).

The concurrence of an extrapulmonary source of infection with contiguous septic

thrombophlebitis complicated by septic pulmonary embolism seems to affect particularly the adult populations. A high index suspicion of thrombosis is present in patients where the manifestations of the soft tissue infection (erythema, pain, and swelling) can overlap those of SPE (Fred and Harle 1969).

Chest x-ray film could be rather nonspecific, whereas chest CT scan provides the earliest and most easily identifiable indication of SPE and systemic embolization of infection.

Bibliography

Community-Acquired Pneumonia

American Thoracic Society (1995) Hospital-acquired pneumonia in adults: diagnosis, assessment of severity, initial antimicrobial therapy and preventive strategies. Am J Respir Crit Care Med 153:1711–1719

Aquino SL, Gamsu G, Webb WR et al (1996) Tree-in-bud pattern. Frequency and significance on thin section CT. J Comput Assist Tomogr 20:594–599

Austin JH, Muller NL, Friedman PJ et al (1996) Glossary of terms for CT of the lungs: recommendations of the Nomenclature Committee of the Fleishner Society. Radiology 200:327–331

Barlett JG, Finegold SM (1974) Anaerobic infections of the lung and pleural space. Am Rev Respir Dis 110:56–77

Bhalla M, Mc Loud TC (1998) Pulmonary infections in the normal host. In: Mc Loud TC (ed) Thoracic radiology, the requisites. Mosby, Philadelphia

Chastre J, Trouillet H, Vuagnat A et al (1998) Nosocomial pneumonia in patient with acute distress respiratory syndrome. Am J Respir Crit Care Med 157:1165–1172

De Paso WJ (1991) Aspiration pneumonia. Clin Chest Med 12:269–284

Franquet T (2001) Imaging of pneumonia: trends and algorithms. Eur Respir J 18:196–208

Hansell DM, Bankier AA, MacMahon H et al (2008) Fleischner Society: glossary of terms for thoracic imaging. Radiology 246:697–722

Heussel CP, Kauczor HU, Heussel G et al (1997) Early detection of pneumonia in febrile neutropenic patients. Use of thin section CT. AJR Am J Roentgenol 169:1347–1353

Ito I, Ishida T, Togashi K et al (2009) Differentiation of bacterial and non bacterial community-acquired pneumonia by thin-section computed tomography. Eur J Radiol 72(3):388–395

Kofteridis D, Samonis G, Mantadakis E et al (2009) Respiratory tract infections caused by Haemophilus influenzae: clinical features and predictors of outcome. Med Sci Monit 15:135–139

Marom EM, McAdams HP, Erasmus JJ et al (1999) The many faces of pulmonary aspiration. AJR Am J Roentgenol 172:121–128

Muller NL, Franquet T, Lee KS (2007) Bacterial pneumonia. In: Imaging of pulmonary infections. Lippincott Williams and Wilkins, Philadelphia, pp 20–28

Musher DM, Dowell ME, Shortridge VD (2002) Emergence of macrolide resistance during treatment of pneumococcal pneumonia. N Engl J Med 346:630–631

Naidich DP, McCauley DI, Khouri NF et al (1983) Computed tomography of lobar collapse. J Comput Assist Tomogr 7:745–757

Okada F, Ando Y, Tanque S et al (2012) Radiological findings in acute Haemophilus influenzae pulmonary infection. Br J Radiol 85:121–126

Primack SL, Hartman TE, Lee KS et al (1994) Pulmonary nodules and the CT halo sign. Radiology 190:513–515

Reittner P, Muller NL, Heyneman L (2000a) Mycoplasma pneumoniae pneumonia: radiographic and high resolution CT features in 28 patients. AJR Am J Roentgenol 174:37–41

Shiley KT, Van Deerlin VM, Miller WT (2010) Chest CT features of community-acquired respiratory viral infections in adult patients with lower respiratory tract infections. J Thorac Imaging 25(1):68–75

Thurlbeck WM, Miller RR, Muller NL, Rose S III (1991) Diffuse diseases of the lung: a team approach. BC Decker/Mosby Year Book, Philadelphia, pp 65–92

Vilar J, Domingo ML, Soto C et al (2004a) Radiology of bacterial pneumonia. Eur J Radiol 51:102–113

Vincent JL, Bihari DJ, Suter PM et al; EPIC International Advisory Committee (1995) The prevalence of nosocomial infection in intensive-care Units in Europe. Results of the European prevalence of infections in intensive care (EPIC) study. JAMA 274:639–644

Winer-Muram HT, Rubin SA, Ellis JV et al (1993) Pneumonia and ARDS in patients receiving mechanical ventilation: diagnostic accuracy of chest radiography. Radiology 188:479–485

Atypical Infections

Aquino SL, Dunagan DP, Chiles C, Haponik EF (1998) Herpes simplex virus 1 pneumonia: patterns on CT scans and conventional chest radiographs. J Comput Assist Tomogr 22(5):795–800

Arnold FW, Summersgill JT, Lajoie AS, Peyrani P, Marrie TJ, Rossi P et al (2007) A worldwide perspective of atypical pathogens in community-acquired pneumonia. Am J Respir Crit Care Med 175(10):1086–1093

Becroft DM (1967) Histopathology of fatal adenovirus infection of the respiratory tract in young children. J Clin Pathol 20(4):561–569

Boroja M, Barrie JR, Raymond GS (2002) Radiographic findings in 20 patients with Hantavirus pulmonary syndrome correlated with clinical outcome. AJR Am J Roentgenol 178(1):159–163

Chan MS, Chan IY, Fung KH, Poon E, Yam LY, Lau KY (2004) High-resolution CT findings in patients with severe acute respiratory syndrome: a pattern-based approach. AJR Am J Roentgenol 182(1):49–56

Chong S, Lee KS, Kim TS, Chung MJ, Chung MP, Han J (2006) Adenovirus pneumonia in adults: radiographic and high-resolution CT findings in five patients. AJR Am J Roentgenol 186(5):1288–1293

Cunha CB (2010) The first atypical pneumonia: the history of the discovery of Mycoplasma pneumoniae. Infect Dis Clin North Am 24(1):1–5

Drysdale SB, Green CA, Sande CJ (2016) Best practice in the prevention and management of paediatric respiratory syncytial virus infection. Ther Adv Infect Dis 3(2):63–71

Eaton MD, Meiklejohn G, van Herick W (1944) Studies on the etiology of primary atypical pneumonia : a filterable agent transmissible to cotton rats, hamsters, and chick embryos. J Exp Med 79(6):649–668

Fairbank JT, Patel MM, Dietrich PA (1991) Legionnaires' disease. J Thorac Imaging 6(3):6–13

Fields BS, Benson RF, Besser RE (2002) Legionella and Legionnaires' disease: 25 years of investigation. Clin Microbiol Rev 15(3):506–526

Franquet T (2011) Imaging of pulmonary viral pneumonia. Radiology 260(1):18–39

Franquet T, Lee KS, Muller NL (2003) Thin-section CT findings in 32 immunocompromised patients with cytomegalovirus pneumonia who do not have AIDS. AJR Am J Roentgenol 181(4):1059–1063

Fraser DW, Tsai TR, Orenstein W, Parkin WE, Beecham HJ, Sharrar RG et al (1977) Legionnaires' disease: description of an epidemic of pneumonia. N Engl J Med 297(22):1189–1197

Gasparetto EL, Davaus T, Escuissato DL, Marchiori E (2007) Hantavirus pulmonary syndrome: high-resolution CT findings in one patient. Br J Radiol 80(949):e21–e23

Graham BS, Snell JD Jr (1983) Herpes simplex virus infection of the adult lower respiratory tract. Medicine (Baltimore) 62(6):384–393

Guckel C, Benz-Bohm G, Widemann B (1989) Mycoplasmal pneumonias in childhood. Roentgen features, differential diagnosis and review of literature. Pediatr Radiol 19(8):499–503

Hahn DL (1999) Chlamydia pneumoniae, asthma, and COPD: what is the evidence? Ann Allergy Asthma Immunol 83(4):271–288, 91; quiz 91–92

Hsieh SC, Kuo YT, Chern MS, Chen CY, Chan WP, Yu C (2007) Mycoplasma pneumonia: clinical and radiographic features in 39 children. Pediatr Int 49(3):363–367

John SD, Ramanathan J, Swischuk LE (2001) Spectrum of clinical and radiographic findings in pediatric mycoplasma pneumonia. Radiographics 21(1):121–131

Karnak D, Beng-sun S, Beder S, Kayacan O (2001) Chlamydia pneumoniae infection and acute exacerbation of chronic obstructive pulmonary disease (COPD). Respir Med 95(10):811–816

Kim JS, Ryu CW, Lee SI, Sung DW, Park CK (1999) High-resolution CT findings of varicella-zoster pneumonia. AJR Am J Roentgenol 172(1):113–116

Kim EA, Lee KS, Primack SL, Yoon HK, Byun HS, Kim TS et al (2002) Viral pneumonias in adults: radiologic and pathologic findings. Radiographics 22(Spec No):S137–S149

Kim KW, Goo JM, Lee HJ, Lee HY, Park CM, Lee CH et al (2007) Chest computed tomographic findings and clinical features of legionella pneumonia. J Comput Assist Tomogr 31(6):950–955

Knittler MR, Sachse K (2015) Chlamydia psittaci: update on an underestimated zoonotic agent. Pathog Dis 73(1):1–15

Kruger DH, Ulrich RG, Hofmann J (2013) Hantaviruses as zoonotic pathogens in Germany. Dtsch Arztebl Int 110(27–28):461–467

Kuo CC, Jackson LA, Campbell LA, Grayston JT (1995) Chlamydia pneumoniae (TWAR). Clin Microbiol Rev 8(4):451–461

Manigold T, Vial P (2014) Human hantavirus infections: epidemiology, clinical features, pathogenesis and immunology. Swiss Med Wkly 144:w13937

Marrie TJ, Haldane EV, Noble MA, Faulkner RS, Martin RS, Lee SH (1981) Etiology of atypical pneumonias – a one year prospective study. CMAJ 125:1118–1123

Marrie TJ, Costain N, La Scola B, Patrick W, Forgie S, Xu Z et al (2012) The role of atypical pathogens in community-acquired pneumonia. Semin Respir Crit Care Med 33(3):244–256

Mattar S, Guzman C, Figueiredo LT (2015) Diagnosis of hantavirus infection in humans. Expert Rev Anti Infect Ther 13(8):939–946

Mayer JL, Lehners N, Egerer G, Kauczor HU, Heussel CP (2014) CT-morphological characterization of respiratory syncytial virus (RSV) pneumonia in immune-compromised adults. Rofo 186(7):686–692

McGuinness G, Scholes JV, Garay SM, Leitman BS, McCauley DI, Naidich DP (1994) Cytomegalovirus pneumonitis: spectrum of parenchymal CT findings with pathologic correlation in 21 AIDS patients. Radiology 192(2):451–459

Meyer Sauteur PM, Unger WW, Nadal D, Berger C, Vink C, van Rossum AM (2016) Infection with and carriage of mycoplasma pneumoniae in children. Front Microbiol 7:329

Mohsen AH, McKendrick M (2003) Varicella pneumonia in adults. Eur Respir J 21(5):886–891

Müller NL (2003) Diseases of the lung: radiologic and pathologic correlations. Lippincott Williams & Wilkins, Philadelphia, p 387

Muller NL, Miller RR (1995) Diseases of the bronchioles: CT and histopathologic findings. Radiology 196(1):3–12

Müller NL, Franquet T, Lee KS, Silva CIS (2007) Imaging of pulmonary infections. Lippincott Williams & Wilkins, Philadelphia, p vii,184 p

Murray JF, Mason RJ (2010) Murray and Nadel's textbook of respiratory medicine. Saunders Elsevier, Philadelphia. Available from: http://www.clinicalkey.com/dura/browse/bookChapter/3-s2.0-C20090378058

Oikonomou A, Muller NL, Nantel S (2003) Radiographic and high-resolution CT findings of influenza virus

pneumonia in patients with hematologic malignancies. AJR Am J Roentgenol 181(2):507–511

Okada F, Ando Y, Wakisaka M, Matsumoto S, Mori H (2005) Chlamydia pneumoniae pneumonia and Mycoplasma pneumoniae pneumonia: comparison of clinical findings and CT findings. J Comput Assist Tomogr 29(5):626–632

Peiris JS, Yuen KY, Osterhaus AD, Stohr K (2003) The severe acute respiratory syndrome. N Engl J Med 349(25):2431–2441

Pipavath SJ, Lynch DA, Cool C, Brown KK, Newell JD (2005) Radiologic and pathologic features of bronchiolitis. AJR Am J Roentgenol 185(2):354–363

Ramsey PG, Fife KH, Hackman RC, Meyers JD, Corey L (1982) Herpes simplex virus pneumonia: clinical, virologic, and pathologic features in 20 patients. Ann Intern Med 97(6):813–820

Reimann HA (1938) An acute infection of the respiratory tract with atypical pneumonia. JAMA 111:2377–2384

Reittner P, Muller NL, Heyneman L, Johkoh T, Park JS, Lee KS et al (2000b) Mycoplasma pneumoniae pneumonia: radiographic and high-resolution CT features in 28 patients. AJR Am J Roentgenol 174(1):37–41

Sargent EN, Carson MJ, Reilly ED (1966) Roentgenographic manifestations of varicella pneumonia with postmortem correlation. Am J Roentgenol Radium Ther Nucl Med 98(2):305–317

Simoons-Smit AM, Kraan EM, Beishuizen A, Strack van Schijndel RJ, Vandenbroucke-Grauls CM (2006) Herpes simplex virus type 1 and respiratory disease in critically-ill patients: real pathogen or innocent bystander? Clin Microbiol Infect 12(11):1050–1059

Tsai TF, Finn DR, Plikaytis BD, McCauley W, Martin SM, Fraser DW (1979) Legionnaires' disease: clinical features of the epidemic in Philadelphia. Ann Intern Med 90(4):509–517

Vilar J, Domingo ML, Soto C, Cogollos J (2004b) Radiology of bacterial pneumonia. Eur J Radiol 51(2):102–113

Webb WR, Higgins CB; Ovid Technologies Inc (2011) Thoracic imaging pulmonary and cardiovascular radiology. Wolters Kluwer/Lippincott Williams & Wilkins Health, Philadelphia. Available from: http://ovidsp.ovid.com/ovidweb.cgi?T=JS&PAGE=booktext&NEWS=N&DF=bookdb&AN=01437581/1st_Edition&XPATH=/PG(0)

Yagyu H, Nakamura H, Tsuchida F, Sudou A, Kishi K, Oh-ishi S et al (2003) Chest CT findings and clinical features in mild Legionella pneumonia. Intern Med 42(6):477–482

Tuberculosis

Alkhuja S, Miller A (2001) Tuberculosis and sudden death: a case report and review. Heart Lung 30(5):388–391

American Thoracic Society (1990) Diagnostic standards and classification of tuberculosis. Am Rev Respir Dis 142(3):725–735

Andreu J, Caceres J, Pallisa E, Martinez-Rodriguez M (2004) Radiological manifestations of pulmonary tuberculosis. Eur J Radiol 51(2):139–149

Arora A, Bhalla AS, Jana M, Sharma R (2013) Overview of airway involvement in tuberculosis. J Med Imaging Radiat Oncol 57(5):576–581

Arya M, George J, Dixit R, Gupta RC, Gupta N (2011) Bilateral spontaneous pneumothorax in miliary tuberculosis. Indian J Tuberc 58(3):125–128

Bruzzi JF, Remy-Jardin M, Delhaye D, Teisseire A, Khalil C, Remy J (2006) Multi-detector row CT of hemoptysis. Radiographics 26(1):3–22

Cardinale L, Parlatano D, Boccuzzi F, Onoscuri M, Volpicelli G, Veltri A (2015) The imaging spectrum of pulmonary tuberculosis. Acta Radiol 56(5):557–564

Chatterjee K, Colaco B, Colaco C, Hellman M, Meena N (2015) Rasmussen's aneurysm: a forgotten scourge. Respir Med Case Rep 16:74–76

Cherian G (2004) Diagnosis of tuberculous aetiology in pericardial effusions. Postgrad Med J 80(943):262–266

Corder R (2003) Hemoptysis. Emerg Med Clin North Am 21(2):421–435

European Centre for Disease Prevention and Control (2015) Tuberculosis surveillance and monitoring in Europe 2015 [cited 2016 20.4.2016]. Available from: http://ecdc.europa.eu/en/publications/_layouts/forms/Publication_DispForm.aspx?List=4f55ad51-4aed-4d32-b960-af70113dbb90&ID=1278

Fatimi SH, Javed MA, Ahmad U, Siddiqi BI, Salahuddin N (2006) Tuberculous hilar lymph nodes leading to tracheopulmonary artery fistula and pseudoaneurysm of pulmonary artery. Ann Thorac Surg 82(5):e35–e36

Franquet T, Gimenez A, Cremades R, Domingo P, Plaza V (2000) Spontaneous reversibility of "pleural thickening" in a patient with semi-invasive pulmonary aspergillosis: radiographic and CT findings. Eur Radiol 10(5):722–724

Franquet T, Muller NL, Gimenez A, Guembe P, de La Torre J, Bague S (2001) Spectrum of pulmonary aspergillosis: histologic, clinical, and radiologic findings. Radiographics 21(4):825–837

Glynn JR, Bauer J, de Boer AS, Borgdorff MW, Fine PE, Godfrey-Faussett P et al (1999) Interpreting DNA fingerprint clusters of Mycobacterium tuberculosis. European Concerted Action on Molecular Epidemiology and Control of Tuberculosis. Int J Tuberc Lung Dis 3(12):1055–1060

Halezeroglu S, Okur E (2014) Thoracic surgery for haemoptysis in the context of tuberculosis: what is the best management approach? J Thorac Dis 6(3):182–185

Hammerman KJ, Christianson CS, Huntington I, Hurst GA, Zelman M, Tosh FE (1973) Spontaneous lysis of aspergillomata. Chest 64(6):679–679

Hong SH, Im JG, Lee JS, Song JW, Lee HJ, Yeon KM (1998) High resolution CT findings of miliary tuberculosis. J Comput Assist Tomogr 22(2):220–224

Im JG, Itoh H, Shim YS, Lee JH, Ahn J, Han MC et al (1993) Pulmonary tuberculosis: CT findings – early active disease and sequential change with antituberculous therapy. Radiology 186(3):653–660

Jean-Baptiste E (2000) Clinical assessment and management of massive hemoptysis. Crit Care Med 28(5):1642–1647

Johnson TM, McCann W, Davey WN (1973) Tuberculous bronchopleural fistula. Am Rev Respir Dis 107(1):30–41

Johnston H, Reisz G (1989) Changing spectrum of hemoptysis. Underlying causes in 148 patients undergoing diagnostic flexible fiberoptic bronchoscopy. Arch Intern Med 149(7):1666–1668

Jones BE, Ryu R, Yang Z, Cave MD, Pogoda JM, Otaya M et al (1997) Chest radiographic findings in patients with tuberculosis with recent or remote infection. Am J Respir Crit Care Med 156(4 Pt 1):1270–1273

Khan NA, Akhtar J, Baneen U, Shameem M, Ahmed Z, Bhargava R (2011) Recurrent pneumothorax: a rare complication of miliary tuberculosis. N Am J Med Sci 3(9):428–430

Kim Y, Lee KS, Yoon JH, Chung MP, Kim H, Kwon OJ et al (1997) Tuberculosis of the trachea and main bronchi: CT findings in 17 patients. AJR Am J Roentgenol 168(4):1051–1056

Kim HY, Song KS, Goo JM, Lee JS, Lee KS, Lim TH (2001) Thoracic sequelae and complications of tuberculosis. Radiographics 21(4):839–858; discussion 59–60

Knechel NA (2009) Tuberculosis: pathophysiology, clinical features, and diagnosis. Crit Care Nurse 29(2):34–43; quiz 4

Krishnan B, Shaukat A, Chakravorty I (2009) Fatal haemoptysis in a young man with tuberculous mediastinal lymphadenitis. A case report and review of the literature. Respiration 77(3):333–336

Leung AN (1999) Pulmonary tuberculosis: the essentials. Radiology 210(2):307–322

Leung AN, Muller NL, Pineda PR, FitzGerald JM (1992) Primary tuberculosis in childhood: radiographic manifestations. Radiology 182(1):87–91

Marshall TJ, Jackson JE (1997) Vascular intervention in the thorax: bronchial artery embolization for haemoptysis. Eur Radiol 7(8):1221–1227

Mayosi BM, Burgess LJ, Doubell AF (2005) Tuberculous pericarditis. Circulation 112(23):3608–3616

McGuinness G, Naidich DP, Jagirdar J, Leitman B, McCauley DI (1992) High resolution CT findings in miliary lung disease. J Comput Assist Tomogr 16(3):384–390

Moon WK, Im JG, Yeon KM, Han MC (1997) Tuberculosis of the central airways: CT findings of active and fibrotic disease. AJR Am J Roentgenol 169(3):649–653

Ntsekhe M, Hakim J (2005) Impact of human immunodeficiency virus infection on cardiovascular disease in Africa. Circulation 112(23):3602–3607

Ntsekhe M, Mayosi BM (2013) Tuberculous pericarditis with and without HIV. Heart Fail Rev 18(3):367–373

Odone A, Tillmann T, Sandgren A, Williams G, Rechel B, Ingleby D et al (2015) Tuberculosis among migrant populations in the European Union and the European Economic Area. Eur J Public Health 25(3):506–512

Post FA, Wood R, Pillay GP (1995) Pulmonary tuberculosis in HIV infection: radiographic appearance is related to CD4+ T-lymphocyte count. Tuber Lung Dis 76(6):518–521

Prasad R, Garg R, Singhal S, Srivastava P (2009) Lessons from patients with hemoptysis attending a chest clinic in India. Ann Thorac Med 4(1):10–12

Pratt PC (1979) Pathology of tuberculosis. Semin Roentgenol 14(3):196–203

Remy J, Arnaud A, Fardou H, Giraud R, Voisin C (1977) Treatment of hemoptysis by embolization of bronchial arteries. Radiology 122(1):33–37

Remy J, Smith M, Lemaitre L, Marache P, Fournier E (1980) Treatment of massive hemoptysis by occlusion of a Rasmussen aneurysm. AJR Am J Roentgenol 135(3):605–606

Reuter H, Burgess LJ, Doubell AF (2005) Role of chest radiography in diagnosing patients with tuberculous pericarditis. Cardiovasc J S Afr 16(2):108–111

Revel MP, Fournier LS, Hennebicque AS, Cuenod CA, Meyer G, Reynaud P et al (2002) Can CT replace bronchoscopy in the detection of the site and cause of bleeding in patients with large or massive hemoptysis? AJR Am J Roentgenol 179(5):1217–1224

Rozenshtein A, Hao F, Starc MT, Pearson GD (2015) Radiographic appearance of pulmonary tuberculosis: dogma disproved. AJR Am J Roentgenol 204(5):974–978

Santelli ED, Katz DS, Goldschmidt AM, Thomas HA (1994) Embolization of multiple Rasmussen aneurysms as a treatment of hemoptysis. Radiology 193(2):396–398

Sepkowitz KA (1996) How contagious is tuberculosis? Clin Infect Dis 23(5):954–962

Sharma N, Kumar P (2002) Miliary tuberculosis with bilateral pneumothorax: a rare complication. Indian J Chest Dis Allied Sci 44(2):125–127

Sharma SK, Mohan A, Sharma A (2012) Challenges in the diagnosis & treatment of miliary tuberculosis. Indian J Med Res 135(5):703–730

Singh AS, Atam V, Das L (2014) Secondary spontaneous pneumothorax complicating miliary tuberculosis in a young woman. BMJ Case Rep 2014

Song JW, Im JG, Shim YS, Park JH, Yeon KM, Han MC (1998) Hypertrophied bronchial artery at thin-section CT in patients with bronchiectasis: correlation with CT angiographic findings. Radiology 208(1):187–191

Suchet IB, Horwitz TA (1992) CT in tuberculous constrictive pericarditis. J Comput Assist Tomogr 16(3):391–400

Uflacker R, Kaemmerer A, Neves C, Picon PD (1983) Management of massive hemoptysis by bronchial artery embolization. Radiology 146(3):627–634

van Crevel R, Ottenhoff TH, van der Meer JW (2002) Innate immunity to Mycobacterium tuberculosis. Clin Microbiol Rev 15(2):294–309

Woodring JH, Vandiviere HM, Fried AM, Dillon ML, Williams TD, Melvin IG (1986) Update: the radiographic features of pulmonary tuberculosis. AJR Am J Roentgenol 146(3):497–506

World Health Organization (2015) 20th edition of WHO global TB report. [updated 20.4.2016]. Available from: http://www.who.int/tb/publications/global_report/en/

Yilmaz MU, Kumcuoglu Z, Utkaner G, Yalniz O, Erkmen G (1998) Computed tomography findings of tuberculous pleurisy. Int J Tuberc Lung Dis 2(2):164–167

Yoon W, Kim JK, Kim YH, Chung TW, Kang HK (2002) Bronchial and nonbronchial systemic artery embolization for life-threatening hemoptysis: a comprehensive review. Radiographics 22(6):1395–1409

Hematogenous Spread of Pulmonary Infection

Angus DC, van der Poll T (2013) Severe Sepsis and septic shock. N Engl J Med 369:840–841

Baddour LM, Betmann MA, Bolger AF et al (2003) Non valvular-cardiovascular device-related infections. Circulation 108:2015–2031

Balakrishnan J, Meziane MA, Siegelman SS et al (1989) CT appearance with pathological correlation. J Comput Assist Tomogr 13(6):941–945

Boyle-Vavra S, Daum RS (2006) Community-acquired methicillin-resistant Staphylococcus aureus: the role of Panton-Valentine leukocidin. Lab Invest 87(1):3–9

Boyle-Vavra S, Daum RS (2007) Community-acquired methicillin-resistant S. aureus: the role of Panthon-Valentine leucocidin. Lab Invest 87:3–9

Brenes JA, Goswami U, Williams DN (2012a) The association of septic pulmonary embolism in adults. Oper Respir Med J 6:14–19

Brenes JA, Goswami U, Williams DN (2012b) The association of septic thrombophlebitis with septic pulmonary embolism in adults. Open Respir Med J 6:14–19

Cassling RS, Rogler WC, McManus BM (1985) Isolated pulmonic valve infective endocarditis a diagnostically elusive entity. Am Heart J 109(3):558–567

Chua JD, Wilkoff BL, Lee I et al (2000) Diagnosis and management of infections involving implantable electrophysiologic cardiac devices. Ann Intern Med 133:604–608

Cook RJ, Ashton RW, Aughenbaugh GL et al (2005a) Septic pulmonary embolism: presenting features and clinical course of 14 patients. Chest 128(1):162–166

Cook RJ, Ashton RW, Aughen GL et al (2005b) Septic pulmonary embolism presenting features and clinical course of 14 patients. Chest 128:162–166

Cook RJ, Aschton RW, Aughenbaugh GL (2005c) Septic pulmonary embolism presenting features and clinical course of 14 patients. Chest 128(1):162–166

Farahmand P, Redheuil A, Chauvaud S et al (2011) Images in endovascular medicine: septic pulmonary thromboemboli in an adolescent with Tetralogy of Fallot. Circulation 123:2164–2166

Ferrari AM, Barletta C (2012) Medicina di emergenza urgenza. Il sapere ed il saper fare del medico di emergenza tra linee guida, percorsi clinico assistenziali e rete dell'emergenza. Elsevier, Milano, pp 318–324

Fred HL, Harle TS (1969) Septic pulmonary embolism. Chest 55:483–486

Gadcowski LB, Stout JE (2008) Cavitary pulmonary disease. Clin Microbiol Rev 21(2):305–333

Goldenberg NA, Knapp-Clevenger R, Hays T et al (2005) Lemierre's and Lemierre's-like syndromes in children: survival and thromboembolic outcomes. Pediatrics 116(4):e543–e548

Gorenstem A, Gross E, Houn S et al (2000) The pivotal role of deep vein thrombophlebitis in the development of acute disseminated staphylococcal disease in children. Pediatrics 106, E87

Habib G, Badano L, Tribouilloy C et al (2010) Recommendations for the practise of echocardiography in infective endocarditis. Eur J Echocardiogr 11(2):202–219

Holm K, Frick IM, Bjork L et al (2011) Activation of the contact system at the surface of Fusobacterium necrophorum represents a possible virulence mechanism in Lemierre's syndrome. Infect Immun 79(8):3284–3290

Hota B, Lyles R, Rim J et al (2001) Predictors of clinical virulence in community onset methicillin-resistant S. aureus infections; the importance of USA 300 and pneumonia. Clin Infect Dis 53:766–771

Iwasaki Y, Nagata K, Nakanischi M et al (2001) Spiral CT findings in septic pulmonary emboli. Eur J Radiol 37(3):190–194

Klug D, Lacroix D, Savoye C et al (1997) Systemic infection related to endocarditis on pacemaker leads: clinical presentation and management. Circulation 95:2098–2107

Mac Millan JC, Milstein SH, Samson PC (1978) Clinical spectrum of septic pulmonary embolism and infarction. J Thorac Cardiovasc Surg 75(5):670–679

Melina G, El-Hamamsy I, Sinatra R et al (2010) Late fulminant pulmonary valve endocarditis after the Ross operation. J Thorac Cardiovasc Surg 139(5):e99–e100

Moriera D, Correia E, Rodrigues B (2012) Isolated pulmonary valve endocarditis in an normal hearth. Rev Port Cardiol 31(9):615–617

Nourse C, Starr M, Munckhof W (2007) Community acquired methicillin resistant S. Aureus causes severe disseminated infection and deep venous thrombosis in children: literature review and recommendations for management. J Pediatr Child Health 43:656–661

Nucifora G, Badano L, Hysko F et al (2007) Pulmonary embolism and fever: when should right-sided infective endocarditis be considered? Circulation 115(6):e173–e176

Rossi SE, Goodman PC, Franquet T (2000) Non thrombotic pulmonary embolism. AJR Am J Roentgenol 174(6):1499–1508

Takin R, Acet H, Ertas F (2012) An unusual case of endocarditis: isolated pulmonary valve in patient with patent ductus arteriosus. J Med Cases 3(6):340–343

Uslan DZ, Sohail MR, StSauver JL et al (2007) Permanent pacemaker and implantable cardioverter defibrillator infection: a population-based study. Arch Intern Med 167:669–675

Vinder Have KL, Karmazyn B, Verma M et al (2009) Community acquired methicillin resistant S. aureus in acute musculoskeletal infection in children: a game changer. J Pediatr Orthop 29(8):827–831

Vos FJ, Kullberg BJ, Sturm PD et al (2012) Metastatic infectious disease and clinical outcome in Staphylococcus aureus and Streptococcus species bacteremia. Medicine (Baltimore) 91(2):86–94

Wagenwoort CA (1995) Pathology of pulmonary thromboembolism. Chest 107(1 Suppl):10S–17S

Wang YC, Wang JM, Chow YC et al (2004) Pneumomediastinum and subcutaneous emphysema as the manifestation of emphysematous pyelonephritis. Int J Urol 11:909–911

Yoong KY, Cheong I (1997) A study of Malaysian drug addicts with human immunodeficiency virus infection. Int J STD AIDS 8:118–123